

## AN ABSTRACT OF THE THESIS OF

Theresa Blume for the degree of Master of Science in Bioresource Engineering  
presented on August 21, 2001.

Title: Effect of Salinity on Particle Release and Hydraulic Conductivity in  
Sediments.

Abstract approved:

Signature redacted for privacy.

John S. Selker

Fine particles and colloids, attached to grain surfaces, are abundant in the earth's subsurface. Under certain conditions these particles can be released from the matrix and transported with the mobile phase. One of the mechanisms for sudden particle release is a decrease in groundwater salt concentration below the critical salt concentration (CSC), where repulsion forces between fine particles and matrix surfaces exceed binding forces.

Typically, CSCs are determined with column experiments, where salt solutions with specific concentrations are applied to the matrix of interest. In this study it was attempted to determine the CSC with batch experiments as well as columns. Two types of sediment were tested: (a) pure, mineralogically homogeneous silica sand; and (b) mineralogically heterogeneous sandy sediment, taken from the Hanford formation in southeast Washington. Stepwise decreasing concentrations of salt solution ( $\text{NaNO}_3$ ) were applied until fine particles were released from the

sediments and the CSC was determined. CSCs from batch experiments were compared to those obtained from column experiments, showing that CSCs were determined successfully with this method. It was also found that the amount of particle release, and also the CSC, of the mineralogically heterogeneous Hanford Sediment was generally an order of magnitude higher than for the Silica Sand. The CSC for the Hanford Sediment was found to be 0.1 mol/l  $\text{NaNO}_3$ , which was higher than expected.

Particle release can cause a change in hydraulic conductivity of the matrix, either by washing out the fines and thus increasing the pore sizes, or by plugging of pore constrictions. The phenomenon of permeability changes as a result of particle detachment was investigated in a series of column experiments using coarse and fine sediments from the Hanford Formation in southeast Washington. Columns were subject to a pulse of highly saline solution ( $\text{NaNO}_3$ ) followed by a freshwater shock causing particle release. No permeability decrease occurred within the coarse matrix alone. However, when a thin layer of fine sediment was imbedded within the coarse material (mimicking field conditions at the Hanford Site), permeability decreased significantly during the freshwater shock down to 10 percent of the initial value. The reduction in permeability was shown to be due to occlusion of the fine layer.

Copyright by Theresa Blume

August 21, 2001

All Rights Reserved

**Effect of Salinity on Particle Release and Hydraulic Conductivity in Sediments**

by  
**Theresa Blume**

**A THESIS**

submitted to  
  
**Oregon State University**

in partial fulfillment of  
the requirements for the  
degree of

**Master of Science**

**Presented August 21, 2001**

**Commencement June 2002**

## **ACKNOWLEDGEMENTS**

I would like to thank John Selker without whose support my extended stay at Oregon State University would not have been possible.

Thank you to Noam Weisbrod, who taught me so much. He was always there to listen to me, much more a friend than a professor.

I want to thank Roy Haggerty and Skip Rochefort for serving on my committee.

Thank you to all the people in the Department of Bioresource Engineering, who made me feel at home here, especially David, Melissa and France.

Thank you to Dominik, for being the person that you are, and for proofreading all those drafts.

I also want to thank my parents, Oda and Alfred Blume, who have always supported me in every possible way.

## **CONTRIBUTION OF AUTHORS**

Noam Weisbrod was extensively involved throughout the experimental stages, data analysis, and manuscript preparation. The experiments were performed in the laboratory of John S. Selker, who provided useful suggestions and reviewed the manuscripts.

# TABLE OF CONTENTS

	<u>Page</u>
1 GENERAL INTRODUCTION .....	1
1.1 COLLOIDS AND FINE PARTICLES IN THE SUBSURFACE .....	1
1.1.1 What are Colloids? .....	1
1.1.2 Sources of Mobile Subsurface Colloids .....	2
1.1.3 Typical Research Methodology.....	4
1.1.4 The Importance of Colloids and Fine Particles in the Subsurface .	6
1.2 THE DLVO THEORY .....	10
1.3 THE HANFORD SITE.....	15
1.4 OBJECTIVES.....	16
2 DETERMINATION OF CRITICAL SALT CONCENTRATIONS FOR PARTICLE RELEASE IN HOMOGENEOUS SILICA SAND AND HETEROGENEOUS HANFORD SEDIMENTS.....	17
2.1 ABSTRACT.....	18
2.2 INTRODUCTION.....	19
2.3 THEORY.....	22
2.3.1 DLVO Theory and CSC .....	22
2.3.2 Release Due to Shear Forces .....	25
2.4 MATERIALS AND METHODS.....	27
2.4.1 Sediments and Solutions .....	27
2.4.2 Experimental Procedure .....	29
2.5 RESULTS.....	33
2.5.1 Sediment Properties.....	33
2.5.2 Batch Experiments .....	36

## TABLE OF CONTENTS, CONTINUED

	<u>Page</u>
2.5.3 Column Experiments .....	43
2.5.4 Comparison of CSCs .....	45
2.6 SUMMARY AND CONCLUSIONS .....	47
2.7 ACKNOWLEDGEMENTS .....	48
2.8 REFERENCES .....	50
3 PERMEABILITY CHANGES IN LAYERED HANFORD SEDIMENTS AS A RESULT OF PARTICLE RELEASE .....	54
3.1 ABSTRACT .....	55
3.2 INTRODUCTION .....	56
3.3 THEORY .....	59
3.4 MATERIALS AND METHODS .....	64
3.4.1 Sediments, Glass Beads and Solutions .....	64
3.4.2 Experimental Procedure .....	66
3.5 RESULTS .....	69
3.5.1 Sediment Properties .....	69
3.5.2 Particle Release and Changes in Permeability .....	73
3.6 SUMMARY AND CONCLUSIONS .....	82
3.7 ACKNOWLEDGEMENTS .....	83
3.8 REFERENCES .....	84
4 SUMMARY AND CONCLUSIONS .....	87
5 BIBLIOGRAPHY .....	90
APPENDICES .....	96



## LIST OF FIGURES

<u>Figure</u>	<u>Page</u>
1.1 Size spectrum of colloidal particles (after <i>Stumm</i> 1992).....	2
1.2 The electric double layer. ....	12
1.3 Total interaction energy ( $V_T$ ) as a function of separation distance between colloid and matrix surface. ....	14
2.1 Illustration demonstrating the natural variability of the amounts of fines released from Hanford Sediment (unwashed, < 2mm fraction).. ....	36
2.2 Particle release due to shear stress as a function of shaking time (at 0.82 mol/l $\text{NaNO}_3$ for the Hanford Sediment and 1.17 mol/l $\text{NaNO}_3$ for the Silica Sand). ....	39
2.3 Batch experiment, method I: .....	40
2.4 Batch experiment, method II: .....	42
2.5 Column experiment with (a) Silica Sand and (b) Hanford Sediment: Stepwise decreasing salt concentration and resulting particle release. ....	44
3.1 Hanford Formation: layers of coarse (A) and fine (B) sediment.....	59
3.2 Conceptual diagram of the pore-particle system (after <i>Khilar and Fogler</i> , 1983).....	62
3.3 Experimental set-up.....	67
3.4 Grain size distribution curves for three samples of the Coarse and the two samples of the Fine Sediment.....	72
3.5 Particle size distribution of released particles from the Coarse and the Fine Sediment. ....	73
3.6 Permeability reduction during a freshwater shock.. ....	76

## LIST OF FIGURES, CONTINUED

	<u>Page</u>
3.7 Permeability reduction (overall and in the fine layer segment), and pH changes as a result of freshwater shock (glass bead experiment). ....	78
3.8 Particle release from both sediments as a function of salinity. ....	80
3.9 Outflow Q, EC and pH during a freshwater shock experiment.....	81

## LIST OF TABLES

<u>Table</u>	<u>Page</u>
2.1 Values of $\text{Na}^+$ - CSC found in the literature.....	23
2.2 Chemical analyses and physical properties of the sediments.....	34
2.3 Critical salt concentrations obtained with the three different methods. ....	46
3.1 Chemical analyses and physical properties of the sediments.....	71
3.2 Initial and final values of overall intrinsic permeabilities ( $\text{cm}^2$ ) of 6 experiments. ....	74

## LIST OF APPENDICES

<u>Appendix</u>	<u>Page</u>
A    SCANNING ELECTRON MICROSCOPY: PHOTOGRAPHS OF SEDIMENTS AND ATTACHED PARTICLES.....	97
B    NUMERICAL SIMULATION OF PARTICLE RELEASE FROM SILICA SAND AS A RESULT OF SALINITY CHANGES.....	106

## LIST OF APPENDIX FIGURES

<u>Figure</u>	<u>Page</u>
A.1 SEM pictures of Silica Sand (Accusand <sup>®</sup> 40/50). .....	99
A.2 Surface of Silica Sand (Accusand <sup>®</sup> 40/50) before (A) and after (B) treatment with cycles of salt solution and deionized water. ....	100
A.3 Surface of Silica Sand (Accusand <sup>®</sup> 40/50) after treatment with acid. 101	
A. 4 Grains of the Coarse Hanford Sediment.....	102
A. 5 Surface of Coarse Sediment before (A) and after (B) treatment with cycles of salt solution and deionized water. ....	103
A. 6 Surface of Coarse Sediment after treatment with acid. ....	104
A. 7 Grains of Fine Hanford Sediment. ....	105
B. 1 Conceptual model.....	108
B. 2 Main menu.....	112
B. 3 Input of variables.....	113
B. 4 Initial conditions.....	113
B. 5 Boundary Condition .....	114
B. 6 Model and data of salt concentration in the outflow. ....	115
B. 7 Changing the time-step from 0.3 (model - 1) to 0.08 (model - 2) and the number of nodes from 20 (model - 1) to 80 (model - 2) does not change the output significantly. ....	116
B. 8 Comparison of model output with measured data.....	118

This thesis is dedicated to Oda, Alfred and Johannes.

# EFFECT OF SALINITY ON PARTICLE RELEASE AND HYDRAULIC CONDUCTIVITY IN SEDIMENTS

## 1 GENERAL INTRODUCTION

### 1.1 COLLOIDS AND FINE PARTICLES IN THE SUBSURFACE

#### 1.1.1 What are Colloids?

*“To some the word ‘colloidal’ conjures up visions of things indefinite in shape, indefinite in chemical composition and physical properties, fickle in chemical deportment, things infiltrable and generally unmanageable.” Hedges, 1931*

Colloids are usually defined on the basis of size: at least one dimension is in the size range of 1 nm to 1  $\mu\text{m}$ . Kaolinite plates, for example, typically have only one dimension below the 1  $\mu\text{m}$  limit (Everett 1988). However, these size limits are not rigid and are sometimes extended to particles of up to 10  $\mu\text{m}$  (Stumm 1992). Colloids and fine particles are abundant in soils, sediments and groundwater. The traditional distinction between particulate and dissolved matter (0.45  $\mu\text{m}$  membrane filtration) does not take into account small sized colloids. Due to their small size the surface area per given volume or mass is large ( $> 10 \text{ m}^2/\text{g}$ ) (Kretzschmar *et al.* 1999). High specific surface area results in a high potential for surface-chemical processes such as adsorption of metals, trace elements, radionuclides and other pollutants. Throughout this work colloidal sized particles (up to 10  $\mu\text{m}$ ) will be referred to as “particles”, “fines”, “colloidal particles” or “colloids” in order to

distinguish them from the pore matrix and grain surfaces. Many different kinds of colloids exist in aquatic environments, most of which are presented in **Figure 1.1**.

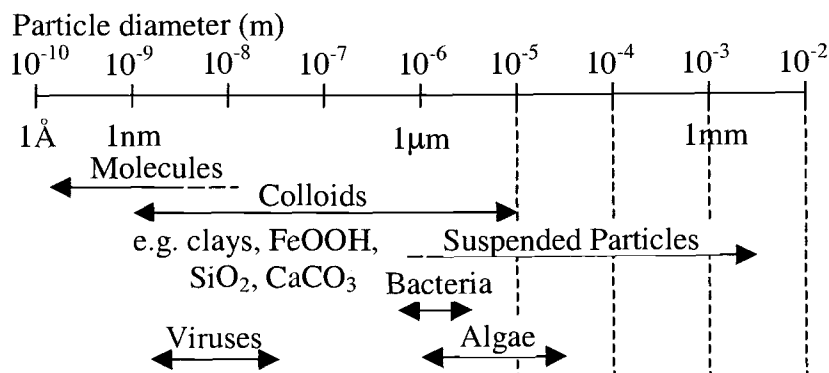


**Figure 1.1** Size spectrum of colloidal particles (after *Stumm* 1992)

Colloids naturally present in soils or sediments are for example clays (kaolinite, illite, smectites and vermiculites), colloidal humic acids, iron hydrous oxides, iron and manganese oxides, and polymeric coatings of soil particles by humus, by hydrous iron (III) oxides and hydroxo-Al(III) compounds. Sometimes biological colloids such as microorganisms and viruses are also present. In anoxic sediments sulfide and polysulfide colloids can also be found (*Stumm* 1992).

### 1.1.2 Sources of Mobile Subsurface Colloids

Colloids can either be attached to matrix surfaces by cementing agents or electrostatic forces; or suspended in water or the permeating solution. Mobile



colloids can be generated by several different mechanisms. One of the possibilities for particle generation is the detachment of colloids from the matrix due to fluid shear forces at high flow rates. This can happen in fracture flow, during rapid rainfall infiltration, and at high pumping rates (*Degueldre et al.* 1989; *Kaplan et al.* 1993; *Ochi and Vernoux* 1998; *Ryan and Gschwend* 1994; *Sharma et al.* 1991). However, in most soils or sediments, flow rates are relatively low, hydrodynamic forces are small and can generally be neglected when compared to other detachment mechanisms (*Cerda* 1987). A second possible mechanism is the detachment of colloids due to changes in solution chemistry, which produce repulsive interactions (e.g. *Grolimund and Borkovec* 1999; *Roy and Dzombak* 1996; *Nightingale and Bianchi* 1977; *Nocito-Gobel and Tobiasson* 1996; *Suarez et al.* 1984; *Kia et al.* 1987; *Kaplan et al.* 1996; *Khilar and Fogler* 1984; *Cerda* 1987). These changes include decreasing ionic strength and increasing pH values. A third way for particles to be released is their detachment due to dissolving cementing agents, which bind the particles to the matrix (*Ryan and Gschwend* 1990). A fourth possibility is in-situ generation as a result of chemical precipitation from the solution. Gradients in geochemical conditions such as groundwater pH, redox potential, ion composition, and CO<sub>2</sub> partial pressure can induce supersaturation and subsequent precipitation. Such gradients can be caused by natural geochemical processes or by contaminant infiltration (*McCarthy and Zachara* 1989; *McCarthy and Wobber* 1993, pp 41-45 and references therein). The introduction of oxygen-rich water into an anoxic aquifer can also result in

precipitation of colloid-sized iron hydroxides (*Liang et al. 1993*). Additionally, colloidal particles containing radionuclides can be formed by weathering of nuclear waste glass in contact with water (*Bates et al. 1992*).

### 1.1.3 Typical Research Methodology

Sampling of mobile colloidal particles from the subsurface is greatly complicated by the need to maintain undisturbed conditions (*Kretzschmar et al. 1999*). Any disturbance of the native conditions can cause particles to release, biasing the samples towards higher colloid concentrations. As a result, special sampling techniques had to be developed that avoided particle generation and mobilization while sampling. One example is passive sampling with the help of dialysis cells (*Weisbrod et al. 1996*). Other methods of sampling groundwater colloids and the problems associated with them are described in *Buffle and van Leeuwen (1993)* (pp 247-315). Sampling mobile colloids in soils and the vadose zone is just as problematical, and few field studies have been published (as reviewed in *Kretzschmar et al. 1999*). One method is the installation of lysimeters, as done by *Kaplan et al. (1996)*, who used a series of lysimeters to determine the release conditions for mobile particles in Ultisol profiles.

To avoid the complications of field sampling many colloid studies have been performed in the lab. Often artificial colloids, such as charged polystyrene or glass microspheres are used (*Sharma et al. 1992*; *Roy and Dzombak 1996*; *Nocito-Gobel and Tobiasson 1996*; *Amirtharajah and Raveendran 1993*). A common laboratory method is the use of columns packed with sediment, soil or glass beads (*Roy and*

*Dzombak 1996; Nocito-Gobel and Tobiason 1996; Ryan and Gschwend 1994; Faure et al. 1996; Amirtharajah and Raveendran 1993; Shainberg et al. 1981).*

Another typical experimental set-up is a core flow unit, where flow through cores of sandstone is established, while chemical or physical conditions are changed (*Khilar and Fogler 1984; Ochi and Vernoux 1998; Mohan et al. 1999; Vaidya and Fogler 1990; Kia et al. 1987*).

Once the mobile colloidal particles are sampled (in the field or in the lab), they need to be characterized. The most important parameters of characterization are: concentration or abundance; composition (mineralogical and chemical); size distribution and particle morphology; and surface characteristics, such as surface area, surface charge, sorption capacity (*Kretzschmar et al. 1999, Buffle and van Leeuwen 1993 (pp 247-315)*). Many methods to determine these parameters exist (*Buffle and van Leeuwen 1993 (pp 247-315)*), only few of which will be mentioned here. Particle concentration can be determined by turbidity or optical absorbance (converted into concentration using a calibration curve), mineralogical composition by X-ray diffraction, and chemical composition by inductively coupled plasma emission spectroscopy (ICP). Optical and scanning electron microscopy (SEM) provides information on particle number, particle morphology, and size. SEM combined with energy dispersive spectroscopy (EDS) may be used to determine element composition either overall or of specific particles. The size distribution can be obtained by diffraction spectroscopy or gravimetrically, while micro-

electrophoresis gives information on average surface charge (*Buffle and van Leeuwen* 1993 (pp 247-315)).

#### 1.1.4 The Importance of Colloids and Fine Particles in the Subsurface

Understanding colloidal transport in the subsurface is essential for assessing the migration of contaminants with low solubility such as radionuclides and hydrophobic organic compounds. Numerous studies have shown that mobile colloids and fine particulate matter are abundant in the subsurface and may facilitate the transport of contaminants that have a high affinity for their surfaces to a much greater extent than predicted by two-phase models (e.g., *Grolimund et al.* 1996; *Kersting et al.* 1999; *Penrose et al.* 1990; *Saiers and Hornberger* 1999). This is promoted by the small size and thus large specific surface area of the colloids, which increases their potential to adsorb contaminants (*Kretzschmar et al.* 1999). *Kersting et al.* (1999) found that plutonium, which has low solubility in water and strong sorption to the solid phase, and is thus traditionally considered relatively immobile in the subsurface, migrated over a distance of at least 1300 m from the location of the nuclear test at the Nevada Test Site. It was shown that 99% of the plutonium isotopes found were associated with colloidal and particulate fractions. In another study at Los Alamos National Laboratory, NM, plutonium was detected downstream of a radioactive waste deposit. Again the plutonium was found to be associated with colloids and migrated as far as 3390 m downstream of its source (*Penrose et al.* 1990). In column experiments it was shown that cesium transport was enhanced by migrating colloids (*Faure et al.* 1996). In this

publication as well as in the study of *Saiers and Hornberger (1999)* cesium transport was significantly accelerated by colloids under conditions of low salinity. This suggests that colloid facilitated transport is strongly dependent on groundwater chemistry. It was also found that sorption of cesium to deposited colloids was substantially less than to mobile colloids. *Puls and Powell (1992)* used arsenate to assess colloid facilitated transport and discovered that the transport rate of colloid-associated arsenate was over 21 times that of the dissolved arsenate. In this study it was also shown that the iron oxide colloids used were not only mobile to a significant extent but were transported faster than the conservative tracer (tritiated water) under certain geochemical conditions. This is explained by size exclusion effects: particles are less subject to diffusion into the small pores and thus more likely to be transported in big pores and preferential flow paths with higher flow velocity. Another suggested explanation is repulsion forces between the colloids and the pore matrix (charge exclusion), which causes the particles to remain at greater distance to the pore wall, thus again being subject to higher flow velocities (*Puls and Powell 1992*). However, the source of these fine mobile particles is often unknown and the particular conditions needed for them to detach from the matrix and become mobile are still an area of active research (*Khilar and Fogler 1998; Kretzschmar et al. 1999; Mohan et al. 1999*).

Researchers from many disciplines have increasingly focused their attention on the causes and consequences of particle release. Changes in pH or in ionic strength may modify the balance between the forces at the particle-grain interface and result

in particle detachment (*Cerda 1987; Khilar and Fogler 1998; Kretzschmar et al. 1999; Vaidya and Fogler 1990*). Once released, the particles can either redeposit on the matrix, be transported with the flow or get entrapped at pore constrictions. As a result permeability can either be increased (by washing out the fines and thus increasing the pore sizes) or decreased (by clogging the pore necks with the fine particles). Whether transport or entrapment occurs is dependent on characteristics of the particles, the matrix, and the solution. Important parameters include the pore structure, the size and concentration of the released particles, the flow velocity, as well as the chemical composition of the liquid phase (*Herzig et al. 1970; Muecke 1979*). *Khilar and Fogler (1998)* distinguished between several different mechanisms of entrapment depending on the ratio of particle size to size of pore constrictions: plugging due to blocking or size exclusion; plugging due to bridging and multiparticle blocking; and plugging due to surface deposition, bridging and multiparticle blocking. This phenomenon and its implications have been observed and studied in many different environments and under different circumstances, such as irrigation of sodic soils (*Frenkel et al. 1978; Pupisky and Schainberg 1979; Shainberg et al. 1981; Quirk and Schofield 1955*), at the seawater-freshwater interface in coastal aquifers (*Goldenberg et al. 1983; Goldenberg et al. 1984*), and during the process of oil extraction where this phenomenon is called 'water sensitivity' and the resulting decrease in hydraulic conductivity is called 'formation damage' (*Baudracco 1990; Khilar and Fogler 1984; Khilar et al. 1983; Kia et al. 1987; Mohan et al. 1999; Mohan et al. 1997; Ochi and Vernoux 1998; Vaidya and*

*Fogler 1990*). *Quirk and Schofield (1955)* showed that the permeability of a silty loam soil declined significantly as soon as the ionic strength dropped below a critical salt concentration. *Frenkel et al. (1978)* found that the observed permeability decrease was due to clogging of pores by dispersed clay particles. The same conclusion was drawn by *Pupisky and Shainberg (1979)*, who also found clay dispersion to be very dependent on the exchangeable sodium percentage (ESP) of the soil. In the study by *Shainberg et al. (1981)* it was further emphasized that even a low ESP can cause decreases in hydraulic conductivity if this soil is leached with rainwater. Another common problem is seawater encroachment into coastal aquifers. The resulting chemical changes as the freshwater-seawater interface is shifting, replacing freshwater with seawater and vice versa can cause significant permeability changes at this interface. This phenomenon was studied with column experiments where aquifer sediments were flushed alternating with seawater and fresh groundwater. The extent of the permeability decrease depended mainly on clay abundance and reached values one to three orders of magnitude lower than the initial hydraulic conductivity (*Goldenberg et al. 1983*). However, one of the most extensively studied phenomena in this context is the so-called formation damage or water sensitivity of sandstone. This is a major concern for the oil and gas producing industry. The injection of solutions during drilling procedures can cause undesirable decreases in flow rates, for example during the exploitation of oil wells. As a result many studies have been done to investigate the causes and possible prevention of the observed permeability reduction (*Baudracco 1990*;

*Khilar and Fogler 1984; Khilar et al. 1983; Kia et al. 1987; Mohan et al. 1999; Mohan et al. 1997; Ochi and Vernoux 1998; Vaidya and Fogler 1990*). The study of sandstone water sensitivity began in the 1940's. Until the 60's it was commonly believed that swelling clays were the major cause of permeability decrease. However, from the 1960's on, clay particle migration was also considered as a potential cause due to the fact that permeability reductions were also observed in sandstone (e.g. Berea sandstone), which contained no swelling clays (*Khilar and Fogler 1984*).

## 1.2 THE DLVO THEORY

Particle release and deposition can be described mathematically by the modified DLVO theory (Derjaguin-Landau-Verwey-Overbeek), which was originally developed in the early 1940's (*Derjaguin and Landau 1941; Khilar and Fogler 1998; Kretzschmar et al. 1999*). According to this theory particles and matrix are subject to a combination of repulsive and attractive forces (including repulsive double layer forces, attractive van der Waals forces, and short range Born repulsion forces). The sum of all these forces or energies is the total interaction energy ( $V_T$ ):

$$V_T = V_A + V_R = V_{LVA} + V_{BR} + V_{DLR} \quad (1)$$

where  $V_A$  is the attractive energy (J),  $V_R$  is the repulsive energy (J),  $V_{LVA}$  is the London-van der Waals energy of interaction (J),  $V_{BR}$  is the Born interaction energy (J), and  $V_{DLR}$  is the double-layer energy of interaction (J) (*Khilar and Fogler 1998*;



*Kretzschmar et al.* 1999). The attractive London-van der Waals interactions are long-range forces, acting over distances of up to 10 nm due to instantaneous dipole-dipole interactions. The magnitude of the London-van der Waals interactions depends for example on polarizability of the surfaces and is generally independent of changes in solution chemistry (*Khilar and Fogler* 1998; *Ryan and Elimelech* 1996). The short-range Born repulsion is due to overlapping electron clouds at very short separation distances. Amphoteric minerals (e.g. iron and aluminum oxyhydroxides) are charged positively at lower pH values and negatively at higher pH while other minerals like clays can have permanent surface charge (usually negative) due to isomorphic substitution (*Ryan and Elimelech* 1996). The charge on particle and grain surfaces causes diffuse double layers, which extend out into the bulk solution (**Figure 1.2**). The resulting double layer repulsion due to overlapping double layers is the third component of the total interaction energy.

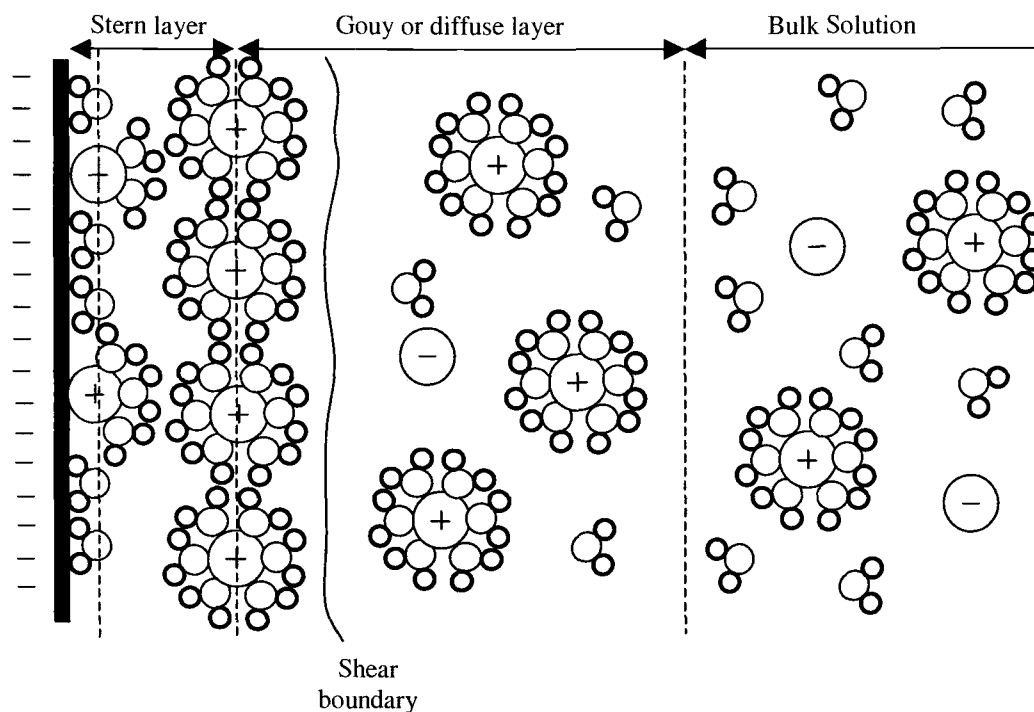


**Figure 1.2** The electric double layer. The Stern layer is subdivided into two sub-layers: an inner layer where specifically adsorbed, unhydrated ions can be found, and an outer region where hydrated counterions are located. The diffuse layer extends out into the bulk solution (after *Elimelech et al. 1995*). (For simplifying purposes, negative ions are not shown as hydrates.)

The ionic strength of the solution controls the extent to which the double layer extends from the surface. At high salt concentrations, the surface charge can be balanced by a thin double layer as the ion concentration near the surface is high. The double layers of approaching surfaces will thus only overlap at very small separation distances and the double layer repulsion is reduced. Decreasing ionic strength will result in expanding double layers and the double layer repulsion will increase consequentially (*Ryan and Elimelech 1996*). **Figure 1.3** shows the

interaction of the energies described above as a function of separation distance between grain surface and particle. The y-axis shows the position of the grain surface. Attraction is depicted as negative, repulsion as positive values. Attached particles will normally be located in the primary minimum where attraction forces are strongest. It can be seen that while the double layer repulsion ( $V_{DLR}$ ) decreases exponentially with separation distance, the London van der Waals attraction decreases only in proportion to  $1/x$  (Ryan and Elimelech 1996). This results in a shallow secondary minimum in the energy profile, which can lead to particle adhesion at larger distances (Stumm 1992).

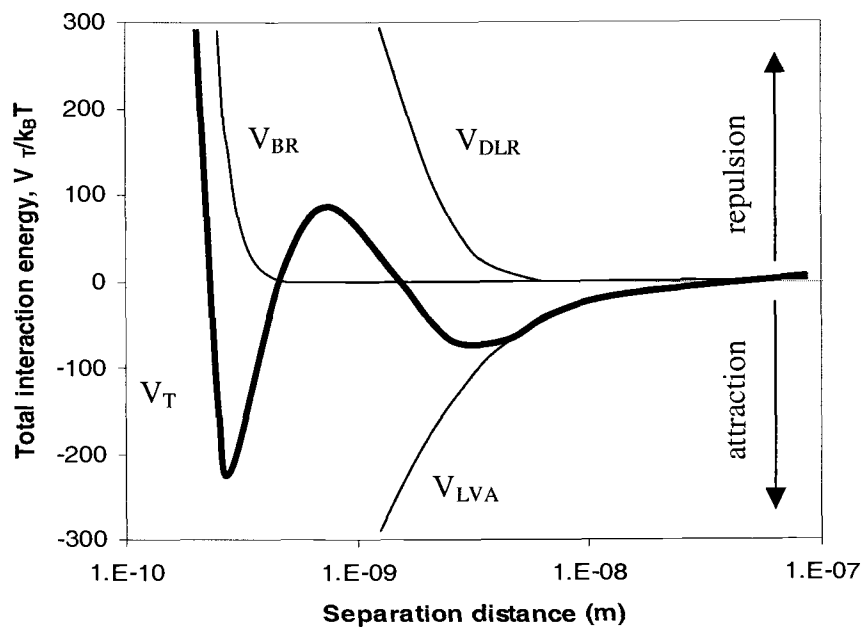


**Figure 1.3** Total interaction energy ( $V_T$ ) as a function of separation distance between colloid and matrix surface. The total interaction energy is the sum of  $V_{DLR}$  (double layer repulsion),  $V_{LVA}$  (London-van der Waals attraction), and  $V_{BR}$  (Born repulsion).  $V_T$  is normalized by  $k_B T$ , which is the product of Boltzmann's constant (J/K) and the absolute Temperature (K) (after *Ryan and Elimelech 1996*).

One possible marker of the Critical Salt Concentration (CSC), at which particles are released from the grain surfaces, is the point at which the primary minimum of the total interaction energy ( $V_T$ ) goes to zero. Assuming the energy barrier (the primary maximum) to be small, it is suggested that the Brownian motion would be enough to cause crossing of this barrier and consequentially detachment (*Khilar and Fogler, 1984*). However, *Khilar and Fogler (1998)* mention that *Mohan (1996)* suggested that the energy barrier could actually prevent

particle release. He determined the CSC as the concentration at which the barrier vanishes.

### 1.3 THE HANFORD SITE

Particle release can be of significant importance at waste deposits such as the Hanford Site in southeast Washington. Here, single shelled tanks filled with highly radioactive waste leaked into the Hanford formation for many years. The leaking waste solution included extremely high concentration of salts ( $> 5 \text{ M Na}^+$ ) as well as radionuclides, other toxic metals, and some organic compounds (GJPO 1996). Recently it was shown that the high surface tension of such extremely saline solution might enhance its downward migration (Weisbrod *et al.* submitted). While migrating in the vadose zone, these hyper-saline solutions (brines) could be diluted dramatically by either mixing with the permeating solution or with condensated water vapor, osmotically derived from the surrounding native sediment (Weisbrod *et al.* 2000). Thus, CSC values at which fine particles (possibly with attached radionuclides) may be mobilized and potential permeability changes of the formation as a consequence of this mobilization are of specific interest in these sediments, as both mechanisms have the potential to influence contaminant transport to a significant extent.

## 1.4 OBJECTIVES

The objective of this study was to investigate the behavior of Hanford Sediments under conditions of changing salinity. This work especially focuses on the determination of critical salt concentrations and changes in hydraulic conductivity. It was attempted to find a method of determining CSCs with batch experiments, which may be cheaper, simpler and less time consuming than column experiments, allowing for more and easier repetitions. Additionally, the particle detachment from Hanford sediments was compared to that of pure silica sand. Potential permeability changes in these sediments of the Hanford Formation due to changes in solution concentration were investigated with column experiments. The Hanford Formation is distinctively layered with more consolidated fine-grained layers, which are generally thinner, alternating with more loose coarse layers, which are generally of greater thickness. As sedimentary basins generally show this characteristic layered pattern, the experiments described here mimic the larger natural system by including a layer of fine sediment imbedded in the coarser sediment in the experimental set-up.

**2 DETERMINATION OF CRITICAL SALT  
CONCENTRATIONS FOR PARTICLE RELEASE IN  
HOMOGENEOUS SILICA SAND AND HETEROGENEOUS  
HANFORD SEDIMENTS**

Theresa Blume, Noam Weisbrod, and John S. Selker

*Department of Bioengineering, Oregon State University, Corvallis, OR, 97331*

## 2.1 ABSTRACT

Fine particles and colloids, attached to grain surfaces, are abundant in the subsurface. Under certain conditions these particles can be released from the matrix and subsequently transported with the mobile phase. One of the mechanisms for sudden particle release is a decrease in groundwater salt concentration to below the critical salt concentration (CSC), where repulsion forces between fine particles and matrix surfaces exceed binding forces.

Typically, CSCs are determined with column experiments, where a sequence of solutions with decreasing concentrations is applied to the matrix of interest. In this study it was attempted to determine the CSC with batch and column experiments. Two types of sediment were tested: (a) pure, homogeneous silica sand; and (b) mineralogically heterogeneous sediment, taken from the Hanford formation in southeast Washington. Stepwise decreasing concentrations of  $\text{NaNO}_3$  solution were applied until fine particles were released from the sediments and the CSC was determined. In the initial batch experiments particle release due to shear stress and the resulting hydrodynamic forces was high, especially for the Hanford Sediment. Two methods were developed to eliminate this effect: (a) post-experimental correction for mechanical effects; and (b) minimizing shear stress on the sediments during the experiment. CSCs from batch experiments were compared to those obtained from column experiments. Our results suggest that CSCs could be determined successfully by batch experiments. It was also found



that both the amount of particle release and the CSC of the Hanford Sediment were an order of magnitude higher than for the Silica Sand.

## 2.2 INTRODUCTION

Understanding colloidal transport in the subsurface is essential for assessing the migration of contaminants with low solubility such as radionuclides and hydrophobic organic compounds. Numerous studies have shown that mobile colloids and fine particulate matter are abundant in the subsurface and may facilitate the transport of contaminants that have a high affinity for their surfaces to a much greater extent than that predicted by two-phase models (e.g., *Kersting et al. 1999; McCarthy and Zachara 1989; Ryan and Elimelech 1996; Saiers and Hornberger 1999; Weisbrod et al. 1996*). However, the source of these fine mobile particles is often unknown and the particular conditions needed for them to detach from the matrix and become mobile are still an area of active research (*Khilar and Fogler 1998; Kretzschmar et al. 1999; Mohan et al. 1999*).

Researchers from many disciplines have increasingly focused their attention on the causes and consequences of particle release. At high flow rates particle release may occur due to the hydraulic shear stress on larger particles (*Kaplan et al. 1993; Khilar and Fogler 1998; Raveendraan and Amirtharajah 1995; Ryan et al. 1998*). In natural systems such as soils, sediments and sandstone, where flow rates are generally low, particle release is more likely to occur due to changes in soil solution/groundwater chemistry (*Cerda 1987; Khilar and Fogler 1984; Khilar and*

Fogler 1998). Particle release can also be caused by a combination of chemical and physical mechanisms (Kaplan *et al.* 1993).

Changes in pH or in ionic strength may modify the balance between the forces at the particle-grain interface and result in particle detachment (Cerdeja 1987; Khilar and Fogler 1998; Kretzschmar *et al.* 1999; Vaidya and Fogler 1990). This phenomenon and its implications have been observed and studied in many different environments and under different circumstances, such as clogging of coastal aquifers (Goldenberg and Magaritz 1984), formation damage during oil exploitation (Khilar and Fogler 1984; Kia *et al.* 1987; Mohan *et al.* 1999), decreasing soil hydraulic conductivity in soils irrigated with sodic waters (Frenkel *et al.* 1978), groundwater turbidity caused by artificial recharge (Nightingale and Bianchi 1977) and contaminant transport (e.g., Amrhein *et al.* 1993; Faure *et al.* 1996; Grolimund *et al.* 1996; Puls and Powell 1992; McCarthy and Zachara 1989; Saiers and Hornberger 1999).

This study focuses specifically on Critical Salt Concentrations (CSCs), the threshold in salinity below which fine particles are released from the matrix surfaces. In ideal, homogenous systems this is likely to be a single value, while heterogeneous systems can lead to range of superimposed CSCs. CSCs can be of significant importance at waste deposits such as the Hanford Site in southeast Washington. Here, single-shelled tanks filled with highly radioactive waste leaked into the Hanford formation for many years. The leaking waste solution included extremely high concentration of salts ( $> 5 \text{ M Na}^+$ ) as well as radionuclides, other

toxic metals, and some organic compounds (*GJPO* 1996). Recently it was shown that the high surface tension of such extremely saline solution might enhance its downward migration (*Weisbrod et al.*, submitted). While migrating in the vadose zone, these hyper-saline solutions (brines) could be diluted dramatically by either mixing with the permeating solution or with condensated water vapor, osmotically derived from the surrounding native sediment (*Weisbrod et al.* 2000). Thus, CSC values at which fine particles with attached radionuclides may be mobilized are of specific interest in these sediments.

CSCs have traditionally been determined through column experiments where solutions of stepwise decreasing salt concentrations were applied to the media until particles were released (*Khilar and Fogler* 1984, *Kia et al.* 1987, *Mohan and Fogler* 1997). Particle release is determined either by the turbidity of the outflow or by a decrease in permeability as particles clog the matrix pores. Media chosen for these experiments are most often glass beads with artificial colloids attached to the beads' surfaces (*Roy and Dzombak* 1996; *Yan et al.* 1995), or cores of Berea Sandstone (*Khilar and Fogler* 1984; *Kia et al.* 1987). In this study it was attempted to find a method of determining CSCs with batch experiments, which may be cheaper, simpler and less time consuming than column experiments, allowing for more and easier repetitions. Batch experiments have been used to determine Critical Flocculation Concentrations (CFCs) of natural colloids and clays (*Kaplan et al.* 1996; *Miller et al.* 1990) but our literature study did not reveal comparable studies for the inverse case of particle release from natural sediment. The CSC

determined for Hanford sediment was compared to the CSC determined for pure silica sand, and differences and similarities were analyzed.

## 2.3 THEORY

### 2.3.1 DLVO Theory and CSC

According to the modified DLVO theory (Derjaguin-Landau-Verwey-Overbeek), particles and matrix are subject to a number of repulsive and attractive forces (e.g. repulsive double layer forces, attractive van der Waals forces, short range Born repulsion forces), the sum of which is the total interaction energy ( $V_T$ ):

$$V_T = V_A + V_R = V_{LVA} + V_{BR} + V_{DLR} \quad (1)$$

where  $V_A$  is the attractive energy (J),  $V_R$  is the repulsive energy (J),  $V_{LVA}$  is the London-van der Waals energy of interaction (J),  $V_{BR}$  is the Born interaction energy (J), and  $V_{DLR}$  is the double-layer energy of interaction (J) (*Khilar and Fogler 1998; Kretzschmar et al. 1999*). High salt concentration results in increasing attraction forces between the matrix and the fine particles attached to its surface. For particles to be released, a higher energy barrier has then to be overcome. A decrease in ionic strength results in a decreasing height of this energy barrier until the CSC is reached, the energy barrier reduces to zero and repulsion forces dominate, causing the attached particles to be released (*Khilar and Fogler 1984; Kretzschmar et al. 1999*). *Kallay et al. (1986, 1987)* noted that under very specific conditions, and for a very low salinity range, particle detachment could also be

enhanced with increasing salt concentrations. This corresponds with a double-layer undergoing relaxation in the case of particle release. However, this situation is limited to constant potential conditions and is an exception (*Kallay et al.* 1986; 1987).

CSCs are not only different from sediment to sediment (soil to soil) but are also dependent on valency and size of the cation of the salt. Polyvalent ions (e.g.  $\text{Ca}^{2+}$ ) are more strongly adsorbed to the matrix surfaces than monovalent ions and thus are less likely to be removed by the fresh water pulse or require lower CSCs. Within the same valency the larger ions (e.g.  $\text{Cs}^+$  compared to  $\text{Na}^+$ ) experience stronger sorption. The most commonly applied salt in experiments determining the CSC is NaCl, a monovalent dispersive salt. A number of CSC values found in the literature are shown in **Table 2.1**.

**Table 2.1** Values of  $\text{Na}^+$  - CSC found in the literature. (Note that *Grolimund et al.* 1998 determined the critical deposition concentration, which is marked by a sudden decrease in deposition rate.)

Authors	Matrix used	CSC ( $\text{Na}^+$ )
Khilar and Fogler 1984	Berea Sandstone	0.07 M
Kia et al. 1987	Berea Sandstone	0.03-0.04 M
Grolimund et al. 1998	Silty Loam Soil	0.2 M
Quirk and Schofield 1955	Silty Loam Soil	0.25 M
Mohan and Fogler 1997	Stevens Sandstone	0.25 M

*Khilar and Fogler* (1984) determined CSCs of Berea Sandstone for a number of other salts and showed that, as expected from the theory, columns saturated with divalent salt like  $\text{Ca}^{2+}$  show almost no particle release and the CSC is at concentration of less than 0.0001 M. Within the monovalent salts, which generally generate higher particle release, CSCs range from 0.006 M for CsCl to 0.07 M for NaCl and LiCl. The CSCs can be placed in the following order from high to low, depending on the cation of the salt solution:  $\text{Na}^+$ ,  $\text{Li}^+$  >  $\text{K}^+$  >  $\text{NH}_4^+$  >  $\text{Cs}^+$  (*Khilar and Fogler* 1984). Additionally, the magnitude and nature of prior particle deposition also has an effect on particle release (*Nocito-Gobel and Tobiason* 1996).

Swelling clays, such as montmorillonite, can also induce migration of fines. This refers to dislocation of fines that are in contact with the swelling clay as a result of the sudden expansion during a transition in swelling regime from crystalline to osmotic swelling. Crystalline swelling is a result of the hydration of the cation, while osmotic swelling is usually explained with the expanding double layers according to the DLVO theory (see *Mohan and Fogler* (1997) for details). In the crystalline regime the spacing of the clay platelets is increased in discrete increments as water layers are incorporated as a result of decreasing salinity. The transition to osmotic swelling is marked by a large discrete jump in spacing of clay platelets, after which the separation distance is a continuous function of the salt concentration of the permeating liquid (*Mohan et al.* 1999; *Mohan and Fogler*, 1997). This transition is attributed to a specific salt concentration, which can also be called CSC. The CSC for Stevens sandstone, which contains swelling clays was

found to be an order of magnitude higher than CSC values for Berea sandstone, which does not contain swelling clays (*Mohan and Fogler 1997*).

### 2.3.2 Release Due to Shear Forces

During infiltration in soil/sediment, hydrodynamic shear forces are often assumed to be negligible concerning particle release. However, this is not the case when agitating sediment samples in a liquid phase, as in the batch experiments described in the section 2.4.2.1. During the shaking process particles are detached from the grain surfaces due to changes in salinity and by the hydrodynamic shear forces resulting from agitation.

Fluid shear rate ( $G$ ), lift force ( $F_L$ ), and fluid drag force ( $F_D$ ) were roughly estimated using the approach of *Bergendahl and Grasso (1998)*. The fluid shear rate can be estimated with the following equations:

$$G = \sqrt{\frac{\varepsilon}{\nu}} \quad (2)$$

where  $G$  is the fluid shear rate ( $s^{-1}$ ),  $\varepsilon$  is the rate of kinetic energy dissipation per mass of fluid ( $J/kg \ s$  or  $cm^2/s^3$ ), and  $\nu$  the fluid kinematic viscosity ( $cm^2/s$ ) =  $1.004 \cdot 10^{-2} \text{ cm}^2/s$  (water at  $20^\circ C$ ). The rate of energy dissipation may be estimated using

$$\varepsilon = \frac{[L(1-f)]^2}{\left\{ \frac{T}{\pi} \tan^{-1} \left[ \frac{d}{2L(1-f)} \right] \right\}^3} \quad (3)$$

where  $L$  is the agitation vessel length (cm),  $f$  the fraction of vessel occupied by fluid,  $T$  the rotation period (s) and  $D$  the vessel width (cm) (Bergendahl and Grasso 1998). Although the experimental setup used by Bergendahl and Grasso (1998) was slightly different compared to the setup used in this study, equation (2) was used to get an estimate of the hydrodynamic shear forces in the first set of the batch experiments.

A sphere in slow shear flow is subject to two forces: lift force and drag force, which have the potential of removing the particle from the surface. Inertial effects are neglected in this case (Bergendahl and Grasso 1998). The lift force  $F_L$  can be calculated by using the relationship

$$F_L = \frac{81.2\mu R^3 G^{3/2}}{\nu^{1/2}} \quad (4)$$

where  $F_L$  is the lift force (N),  $\mu$  the absolute viscosity (Pa s),  $R$  the particle radius (m),  $G$  is fluid shear rate ( $s^{-1}$ ), and  $\nu$  is the fluid kinematic viscosity ( $m^2/s$ ) (Bergendahl and Grasso, 1998). The fluid drag force  $F_D$ :

$$F_D = 10.205\pi\mu GR^2 \quad (5)$$

where  $F_D$  is the hydrodynamic drag force (N),  $\mu$  the absolute viscosity (Pa s),  $R$  particle (colloid) radius (m) and  $G$  the fluid shear rate ( $s^{-1}$ ) (Bergendahl and Grasso 1998). The particle Reynolds number was calculated with the following equation:

$$Re_p = \frac{R^2 G}{\nu} \quad (6)$$



where  $Re_p$  is the particle Reynolds number,  $R$  is the particle radius (m),  $G$  is the fluid shear rate ( $s^{-1}$ ) and  $\nu$  is the kinematic viscosity ( $m^2/s$ ) (Bergendahl and Grasso 1998).

## 2.4 MATERIALS AND METHODS

### 2.4.1 Sediments and Solutions

Batch and column experiments were carried out with two types of sediments, (1) a clean silica sand (Accusand<sup>®</sup>, Unimim Corporation, Le Sueur, MN), and (2) a natural sediment taken from the Hanford Formation in southeastern Washington. For this study the 40/50 Accusand<sup>®</sup> grade was used (fraction smaller than sieve #40 (0.42 mm) and larger than sieve #50 (0.30mm), US Standard Sieve System). This almost pure silica sand was chosen for its chemical and physical homogeneity and known composition and properties (Schroth *et al.* 1996). The sediment from the Hanford Formation was chosen due to the potential importance of colloidal release from these sediments at the Hanford Site. Samples used in this study were obtained 3m below the surface in the 200E Area of the Hanford Site, about 1km from the tank farm.

As this paper focuses on the release of fines originally attached to the sediment grain surfaces, the naturally existing fine fraction within the Hanford sediment was removed by sieving. Only the coarser sand fraction was used ( $> 0.42$  mm and  $< 2$  mm). The sediment was also washed several times with water to eliminate excess

dust particles. Hereafter the pure silica sand (Accusand<sup>®</sup>) will be referred to as "Silica Sand" while the sediment taken from Hanford formation will be referred to as "Hanford Sediment."  $\text{NaNO}_3$ , the major salt in the wastes leaking from the Hanford tanks, was used for these experiments in solutions with a range of concentrations from 5 mol/l down to about 0.001 mol/l. De-ionized water was used for dilution purposes and no buffer was added. All experiments were conducted at room temperature (20-23°C).

Chemical composition of both sediments was determined by ICP (inductively coupled plasma emission spectroscopy, Perkin and Elmer<sup>®</sup> Optima 3000). Mineralogical composition of the Hanford sediment was determined with X-ray analysis. Sediment samples were hand ground to fine powder using a diamondite mortar and pestle. The powders were mounted into aluminum sample holders against a glass plate, lightly compressed so as to minimize preferred orientation of platy minerals, then analyzed with a computer-assisted Philips XRD 3100 X-ray Diffractometer utilizing monochromatic  $\text{Cu K}\alpha$  radiation (40 kv, 35 ma; quartz reference intensity = 37500 counts/sec). Scans were obtained over an angular 2-theta range of 5-50 degrees with a 0.04 degree step increment and 2 second count time. Digital data were analyzed using Jade 3.1 software. The approximate volume of clay in the suspended fraction was estimated using intensity relations of known clay\quartz\feldspar mixtures. The released fraction of the Hanford sample consisted of fine powder (generally <20- $\mu\text{m}$ ) and was analyzed without further grinding by backloading the powder into aluminum sample holders. Following the

initial analysis, the fine powder was re-suspended in distilled water in a 50-ml centrifuge tube, stirred, and allowed to settle for 5 minutes. The suspended portion was decanted into another centrifuge tube and the fines were concentrated by centrifuging for 10 minutes at 10,000 rpm using a Sorval RC-5B refrigerated centrifuge. It can be expected that these concentrated fines consist of the  $<5\text{-}\mu\text{m}$  component of the original dispersed particles. A sample of this material was prepared for XRD analysis by smearing the clay onto a glass slide and drying at room temperature.

Particle size distributions for the released particles were determined by sequential filtration of 10 ml solution through a Millipore® Swinnex-25 filtration device with Nuclepore® polycarbonate membrane filters with pore sizes of 10, 8, 5, 2, 0.4, 0.1  $\mu\text{m}$ . Absorption was measured after each filtration step to estimate to amount of particles in each size class.

## 2.4.2 Experimental Procedure

### 2.4.2.1 Batch Experiments

**Method 1:** 20g of the Silica Sand or 2.5g of the Hanford Sediment respectively were placed in capped 45 ml polypropylene containers and then mixed with 20 ml of highly concentrated saline solution (concentration  $> 1\text{ mol/l NaNO}_3$ ) by shaking it at 150 RPM (lowest setting) for one hour on an Eberbach platform shaker. Particle concentration and  $\text{NaNO}_3$  concentration of the supernatant were calculated at the end of this process. Particle concentration was determined from

the absorption of light measured spectro-photometrically with a Bausch and Lomb® Spectronic 21 at 600 nm and converted to particle concentration using a calibration curve. A linear correlation was found for both sediments between absorption values and particle concentration (g/l) of the detached particles from 0.05 to 1 mg/ml.  $\text{NaNO}_3$  concentration was determined from EC, which was measured with a GLA® Instant EC Salinity Drop Tester. A calibration curve between EC and  $\text{NaNO}_3$  concentration was obtained from 0 to 5 mol/l. In the case of the Hanford Sediment, the amount of sediment per sample was reduced to 2.5 g in order to keep the absorption values within the measuring range of the spectrophotometer. After taking these measurements the supernatant was removed. New solution with lower salinity was added to the sediment sample and then put on the shaker for 1 h before measuring EC and light absorption again. The process was repeated several times while decreasing the ionic strength of the newly added solution stepwise from 1.2 mol/l down to 0.002 mol/l (the resulting concentrations were 1.2, 0.41, 0.16, 0.08, 0.03, 0.015, 0.002 and 1.17, 0.4, 0.23, 0.17, 0.11, 0.06, 0.003 mol/l for the Silica Sand and Hanford Sediment, respectively). The high variance in released amounts of fines, due to sample-to-sample variability was the rationale for choosing this experimental method, where a series of salt concentrations is applied to the same sediment sample rather than taking a new sample for each concentration. This decreases the effect of sample-to-sample variability within a single series. The concentration of released particles at each step decreases with increasing number of increments as a result of dilution.

Consequently it was necessary to limit the number of steps to stay within the measuring range of the spectrophotometer. Each series usually consisted of 5 repetitions.

Two methods were used to address the possibility of mechanical particle release due to shear stress (resulting from the shaking procedure). For the first set of experiments mechanical release was determined with a separate experiment where the sample was agitated continuously while salinity was kept constant above the CSC (at  $\sim 1 \text{ mol/l} \pm 0.17$ ). Chemical release (induced by changes in solution chemistry) is assumed to be zero at these high salt concentrations. Consequently the release observed must be due to shear stress. A simple logistic function was fitted to the data and then used to model mechanical release over time. Finally, the calculated mechanical release, based on the model, was subtracted from overall particle release in the experiments described above, delivering values for release due only to variations in ionic strength of the solution. Results obtained with this method were then compared to the second set of batch experiments described below.

**Method 2:** The second set of experiments was carried out using essentially the same set-up as described above. Again, salt concentration was decreased stepwise resulting in the following concentrations: 1.19, 0.28, 0.10, 0.034, 0.02, 0.012, 0.002 mol/l for the Silica Sand and 1.6, 1.2, 0.7, 0.3, 0.22, 0.15, 0.11, 0.10, 0.05, 0.02, 0.012, 0.002, 0.001 mol/l (combining several series) for the Hanford Sediment. Instead of subtracting mechanically derived particle release afterwards,

these effects were prevented during the shaking process. This was achieved by fitting a circular metal mesh (stainless steel, 0.25 mm openings, 30 mm diameter) into the polypropylene container so that the sediment was contained in place and no longer moved with the solution during the shaking process. As a result, shear forces acting on the sediment grains were reduced considerably and could now be neglected assuming that all detached particles are the result of chemical release only. Each series was run in 4 repetitions. An additional sample with constant salinity ( $\sim 1$  mol/l) was used as a control to confirm the negligibility of mechanical release.

#### 2.4.2.2 Column Experiments

The column experiments were carried out with both Silica Sand and Hanford Sediment. Stepwise decreasing concentrations of  $\text{NaNO}_3$  solution (from 5M to 0.001M) were applied to a sediment column of 5 cm length and 3.5 cm in diameter. Prior to the experiments, the sediment was first saturated with  $\text{CO}_2$  to prevent air bubbles being trapped in the pores. Next, water (low salinity:  $<0.05$  mol/l  $\text{NaNO}_3$ ) was applied slowly from the outlet below the column until the column was saturated. Then, the solution was applied drop-wise from above, each concentration with a total volume of 3 pore volumes. Pore volumes were determined from the amount of water needed to saturate the column. Throughout the experiment flow rates were kept at 1.3-1.4 ml/min. Samples of 9 ml were collected with a fraction collector (Gilson®, Model MFK Fractionator). Particle

concentration (absorption) and EC of the outflow were measured as described in section 2.4.2.1.

#### 2.4.2.3 CSC determination

CSCs are determined as ranges, with the limits of these ranges being the concentrations that were applied; the CSC must fall between these values. This critical range was determined by calculating the slopes of the release functions. The criterion of beginning particle detachment was an increasing slope ( $(P_{C2}-P_{C1})/C_1-C_2$ , where  $P_{C1}$  is the detached particle concentration at salt concentration  $C_1$  and  $P_{C2}$  at salt concentration  $C_2$ ) to a value of 2 or more. When more than one set of batch experiments was run, the resulting ranges were overlain and the maximum lower and minimum upper boundary were determined. For the column experiments the CSCs were determined by the first sharp increase of particle concentration at the beginning of the peak.

## 2.5 RESULTS

### 2.5.1 Sediment Properties

The sediment taken from the Hanford Formation is mineralogically heterogeneous, while the Silica Sand was chosen for its known mineralogical homogeneity (essentially pure quartz), low traces of metals and uniform shape and particle size (**Table 2.2**) (*Schroth et al.* 1996). The  $d_{60}/d_{10}$  value (uniformity

coefficient) of the Hanford Sediment was 3.03, compared to 1.20 for the Silica Sand (*Schroth et al.* 1996), illustrating the significant contrast between the physical properties of the heterogeneous and homogeneous sediment.

**Table 2.2** Chemical analyses and physical properties of the sediments.

Sediment	K ppm	Ca meq/100g	Mg meq/100g	Na meq/100g	Mn ppm	Fe ppm	d <sub>60</sub> /d <sub>10</sub>	d <sub>50</sub> mm
Silica Sand	39	<0.1	<0.1	<0.1	0.1	2.5	1.20	0.36
Hanford Sediment	121	4.9	1.4	0.63	0.4	4.6	3.03	0.67

The mineralogy of the Hanford Sediment is dominated by anorthitic plagioclase and ferromagnesian minerals common to basalt (augite and hornblende). Quartz is a relatively minor component of the Hanford Sediment, reflecting the absence of this mineral in basalt. Clay minerals are only a trace component and include mica (biotite and muscovite). In general, the clay mineral content as measured with X-ray diffraction is <10% and probably represents undispersed mud fragments or cemented soil clasts, while the clay size fraction is < 1%. The released particles of the Hanford Sediment consist of a mixture of clay and non-clay minerals. The clay mineral assemblage includes smectite (montmorillonite), mica (most likely muscovite and biotite), chlorite, and kaolinite.



Mica appears to dominate the clay assemblage of both the <20- and <5- $\mu\text{m}$  fractions, but smectite is generally enriched in the finer sediment concentrate. Clay minerals compose about 40-50% of the detached particles, although clays are more abundant in the <5- $\mu\text{m}$  fraction (60-70%). The non-clay fraction includes quartz, Ca-rich plagioclase, augite, hornblende, traces of K-feldspar, and iron oxides. Quartz abundance exceeds that of plagioclase and may represent glacial silt derived from the upper Columbia River basin during episodic glacial outburst floods.

Mineralogical heterogeneity of the Hanford Sediment, coupled with the small sample size results in significant variations in total particle release from different sediment samples under similar conditions (**Figure 2.1**).

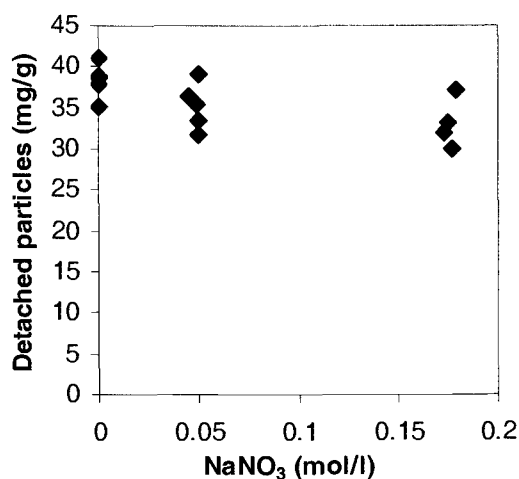


**Figure 2.1** Illustration demonstrating the natural variability of the amounts of fines released from Hanford Sediment (unwashed, < 2mm fraction). Each salt concentration was applied to 5 samples of 2.5g of Hanford Sediment and put on the shaker for 4 hours (mechanical release was not subtracted). Variations of  $\sim \pm 10$  mg/g were found between samples.

Standard deviations of up to 10% (compared to <0.1% for the Silica Sand) were found between samples. The size of the released particles ranged from 0.4-2  $\mu\text{m}$  (~70% of the particles) for the Silica Sand and >2 $\mu\text{m}$  (~80%) for the Hanford Sediment (from sequential filtration of column outflow).

## 2.5.2 Batch Experiments

### 2.5.2.1 Release Due to Hydrodynamic Shear Forces

Fluid shear rate, lift force, and drag force for the procedure used in the batch experiments were estimated using equations (2)-(5) and provided the following values: the fluid shear rate  $G = 6400 \text{ s}^{-1}$ , the lift force  $F_L = 3.34 \times 10^{-10} \text{ N}$  and the

fluid drag force  $F_D = 8.25 \times 10^{-10} \text{ N}$  (assuming a particle size of  $2 \mu\text{m}$ ). If the particle size is assumed to be  $1 \mu\text{m}$  these values are  $F_L = 4.18 \times 10^{-11} \text{ N}$  and  $F_D = 2.06 \times 10^{-10} \text{ N}$ . Both drag and lift forces are larger than the values reported by *Bergendahl and Grasso* (1998), as a result of the short rotation period of the shaker, and are likely to have had a significant effect on overall particle release. Particle Reynolds numbers range at about 0.03 to 0.16 for particles the size of 2 and  $5 \mu\text{m}$  respectively, indicating laminar creeping flow around the particles.

*Bergendahl and Grasso* (1998) noted the phenomenon of colloid release as a result of agitation in their study on colloid generation during batch leaching tests. These tests are used to determine the leaching potential of contaminants from soil. Their values for  $0.83 \mu\text{m}$  colloids are several orders of magnitude smaller than the values obtained in our experiments. This is mainly due to the differences in rotation period used (0.4s and 2.0s) leading to a fluid shear rate of  $55 \text{ s}^{-1}$  in their study. *Newman and Stolzenbach* (1996) found that shear stress had an influence on detachment of  $\text{TiO}_2$  colloids from glass beads, especially if there was a sudden increase in shear stress. The shear rates calculated for their system ranged from 3 to  $300 \text{ s}^{-1}$ .

The results of the experiment where particle concentration of the same sample of Hanford Sediment and Silica Sand, respectively, was measured at intervals while continuously agitating it on the shaker also demonstrate the effect of particle release due to shear stress. Particle release in  $\text{mg (released particles)/g (sediment)}$  from the Silica Sand was only about 2% ( $0.5 \text{ mg/g}$ ) of the amount released from the

Hanford Sediment (30 mg/g) (**Figure 2.2**). The slight decrease in amount of particles (from 9.4 mg to 8.8 mg) at the end of the shaking process suggests re-deposition processes in the Silica Sand.

#### 2.5.2.2 Method I: Modeling and Subtracting Mechanical Particle Release

To factor out particle release due to shear stress from overall particle release it was necessary to find a relationship between mechanical release (release due to shaking) and agitation time. This was achieved by fitting the logistic function to the particle release data at high salinity (where chemical release can be neglected) (**Figure 2.2**).

$$N(t) = \frac{N_{\max}}{1 + \left[ \frac{N_{\max}}{N_0} - 1 \right] e^{-kt}} \quad (6)$$

where  $k$  (1/min) is the release rate,  $t$  (min) is time on shaker, and  $N_0$  and  $N_{\max}$  are the initial and maximum amounts of particles that are released/available, respectively.

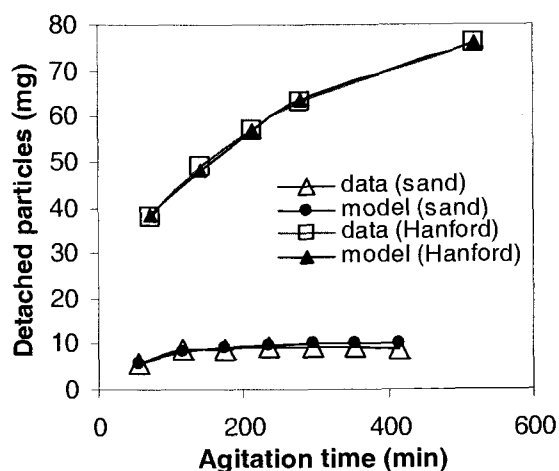


**Figure 2.2** Particle release due to shear stress as a function of shaking time (at 0.82 mol/l  $\text{NaNO}_3$  for the Hanford Sediment and 1.17 mol/l  $\text{NaNO}_3$  for the Silica Sand). A logistic function was fitted to the data (model).

This function seems appropriate as it includes an availability dependent term limiting further release as the number of released particles approaches maximum availability. This maximum availability is equivalent to the carrying capacity used in population models. The model fits with  $R^2$  of 0.923 for the Silica Sand and 0.998 for the Hanford Sediment ( $N_{max} = 10$ ,  $N_0 = 3$ ,  $k = 0.021$  for the Silica Sand and  $N_{max} = 79.29$ ,  $N_0 = 28.78$ ,  $k = 0.007$  for the Hanford Sediment).

The value of mechanical release was subtracted from overall release (while decreasing salinity stepwise) to attain particle release as a function of CSC alone. This procedure was implemented for both sediments (**Figure 2.3**).

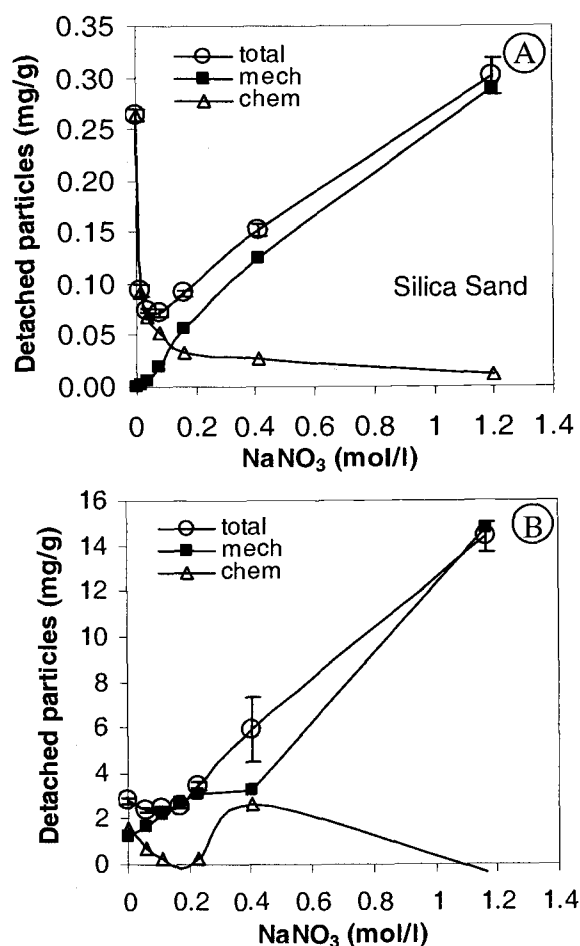


**Figure 2.3** Batch experiment, method I: Total, mechanical and chemical (= total – mechanical) release of particles from (a) Silica Sand; (b) Hanford Sediment. Note that mechanical release depends not on salinity but on the corresponding shaking time given above each data point. Error bars signify  $\pm$  one standard deviation within the set of 5 samples. Further explanation is given in section 2.5.2.2.

For the Silica Sand the CSC obtained was 0.015-0.032 mol/l  $\text{NaNO}_3$  with the amount of chemical release being significantly greater than mechanical release in the vicinity of the CSC. For the Hanford Sediment, the mechanical release was in

the same order of magnitude as the calculated chemical release. This results in high potential error (including negative values and inexplicable trends, see **Figure 2.3**) when subtracting the mechanical from the overall particle release and restricts the ability to accurately determine CSC with this procedure.

#### 2.5.2.3 Method II: Reducing Shear Stress and Mechanical Particle Release

By using a mesh to secure the sediment in place at the bottom of the container the mechanical release was minimized to the point where it could be neglected. The results obtained by this method for the Silica Sand and Hanford Sediment are shown in **Figure 2.4**. Using this method the release curves for the Hanford Sediment showed a much clearer signal attributed to the CSC (**Figure 2.4 (b)**).

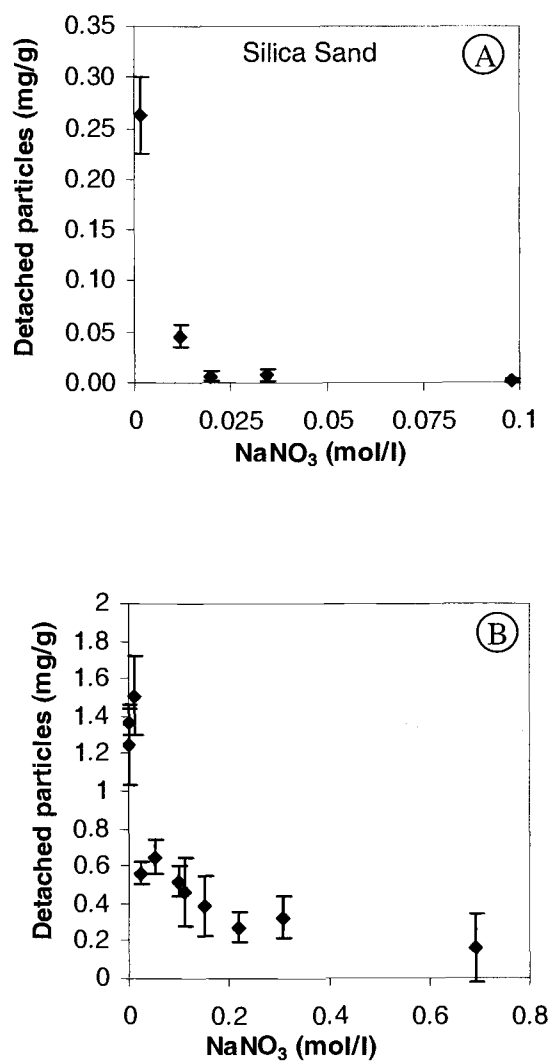


**Figure 2.4** Batch experiment, method II: Particle Release from (a) Silica Sand and (b) Hanford Sediment (average values  $\pm$  one standard deviation).

Note that the values plotted in **Figures 2.4** are typically the averages of 3-4 samples each (in case of the Hanford Sediment the values at salinities of 1.19; 0.15; 0.05; 0.02; 0.0018 mol/l were averages of 6-8 samples each).



The pattern of particle release from the Hanford Sediment suggests bimodal behavior, the final release being preceded by a smaller peak or plateau (**Figure 2.4 (b)**), with a local minimum located at a concentration of  $\sim 0.024$  mol/l  $\text{NaNO}_3$ . The cause for this plateau or secondary peak would require further investigation to be conclusively explained. It is likely due to the heterogeneous mineralogy of the released particles, which includes clay minerals as well as a non-clay fraction (quartz, plagioclase, etc., see section 2.4.2.3). Different fractions of the attached fines with different mineralogy, and thus different chemical properties would be expected to be released at different CSCs causing superposition of several peaks of particle detachment. Further characterization of the detached fines at each salt concentration step would be needed to improve the understanding of this behavior. A possible explanation could also be particle release induced by swelling of montmorillonite, which was observed in Stevens sandstone by *Mohan and Fogler* 1997. Swelling is likely to happen at higher salinities than release due to increasing repulsion forces between fines and the grain surfaces. Montmorillonite is present in the Hanford Sediment, suggesting that this process might also influence the release behavior in our study.

### 2.5.3 Column Experiments

Column experiments were carried out for both sediments in order to compare the CSCs to the results obtained with batch experiments (**Figure 2.5**). A sudden release of fine particles was clearly seen as the salt solution reached the CSC. Note that the broad range in concentrations, which gave rise to minor particle release

seen in the second set of batch experiments with Hanford Sediment was also observed in the column experiments (Figure 2.5 (b)).

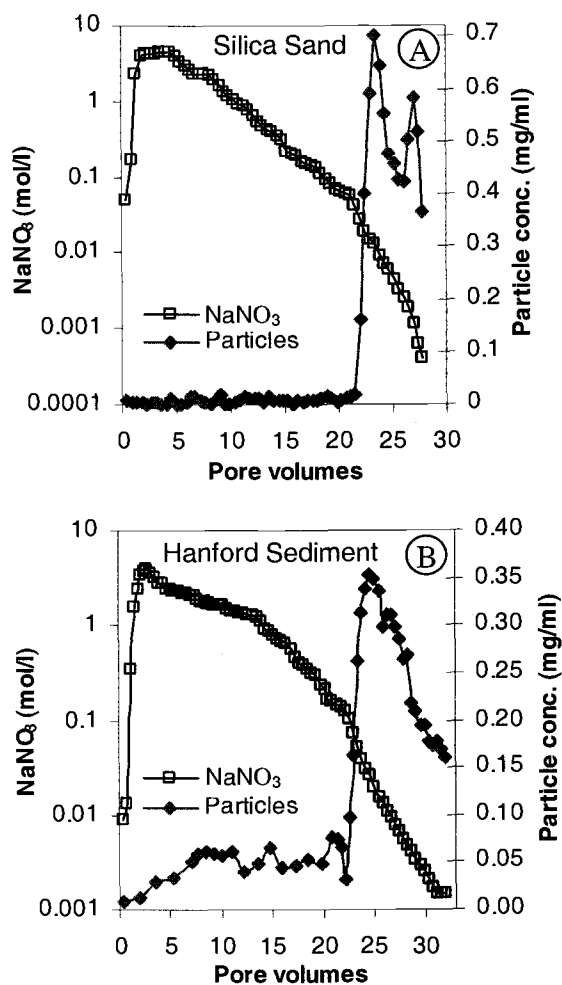


**Figure 2.5** Column experiment with (a) Silica Sand and (b) Hanford Sediment: Stepwise decreasing salt concentration and resulting particle release. Note that minor particle was observed prior to the CSC.

The slight suggestion of a small peak in particle release preceding the final release is not significant considering the scatter in particle concentrations while salinity is still above the CSC. Several repetitions of the experiment would be necessary to distinguish between scatter in concentration values and real phenomena.

#### 2.5.4 Comparison of CSCs

In the first method of batch experiments, mechanical release was subtracted, the resulting particle concentrations were plotted versus time and the CSC was obtained. For the Silica Sand, the average CSC ranged from 0.015-0.032 mol/l, while for the Hanford Sediment the CSC ranged from 0.11-0.17 mol/l  $\text{NaNO}_3$  (**Table 2.3**). In the batch experiments modified to minimize shear stress, particle release due to change in salinity from the Silica Sand started at  $\text{NaNO}_3$  concentrations of 0.015-0.02 mol/l. For the Hanford Sediment the CSC was 0.10-0.11 mol/l  $\text{NaNO}_3$  with a local minimum at  $\sim 0.024$  mol/l (Figure 2.5). The column experiments resulted in CSCs of 0.028 to 0.042 mol/l for the Silica Sand and about 0.12 mol/l for the Hanford Sediment. All values are summarized in **Table 2.3**. Note that the values for the batch experiments are average values, while the column experiment was run without repetition.

**Table 2.3** Critical salt concentrations obtained with the three different methods.

Experiment	Silica Sand	Hanford Sediment
Batch	0.015-0.032 mol/l	0.11-0.17 mol/l
Batch (with mesh)	0.015-0.020 mol/l	0.10-0.11 mol/l
Column	0.028-0.042 mol/l	0.10-0.13 mol/l

CSCs are given in ranges, with the limits of these ranges being the concentrations that were applied; the CSC must fall between these values. The CSC values found for the Hanford Sediment are larger than most values reported in the literature for well defined, ideal systems. However, for natural soils, CSC values of the same order of magnitude were reported by Quirk and Schofield (1955) and Grolimund et al. (1998) (**Table 2.1**). Grolimund et al. (1998) also noted that a quantitative analysis based on the DLVO theory is not considered meaningful for highly heterogeneous natural porous media and in-situ borne fines. The CSC reported by *Mohan and Fogler* (1997) for Stevens sandstone is also high with 0.25 M NaCl. In this case it is attributed to the presence of montmorillonite, which causes particle release due to sudden expansion. As montmorillonite is a component of the Hanford Sediment, this phenomenon could also be a possible explanation for the high CSC value observed here.

The experiments where mechanical release was subtracted also rendered acceptable CSCs. For the Silica Sand, the CSC values covered the range of both values determined using the other methods. Even for the Hanford Sediment, where high mechanical release was masking chemical particle release and making

observations less reliable, the CSC determined was in good agreement with the other results. CSCs of Silica Sand and Hanford Sediment differed by about an order of magnitude. This is likely due to differences in surface chemistry of the matrix and the particles as well as to the availability of particles on the surfaces. For the Hanford Sediment standard deviations amount to 0.1-1.4 mg/g sediment for method 1 and 0.04-0.2 mg/g sediment for method two, while standard deviations of 0.025-0.006 mg/g sediment (method 1) and 0.01-0.038 mg/g sediment (method 2) were found for the Silica Sand.

## 2.6 SUMMARY AND CONCLUSIONS

The three methods used in this study provided similar CSC values for the two sediments, suggesting that batch experiments, especially method 2, are a viable alternative to column-based methods. The advantages of batch experiments include cheaper and simpler experimental set-up, faster repetitions, and greater control of experimental conditions. The minor amount of particle release over a range of salt concentrations above the CSC seen in case of the Hanford Sediment would require further investigation to be conclusively explained; however, it is likely the result of the mineralogically heterogeneous nature of both the sediments and the attached particles. Additionally, the high CSC values observed in the case of the Hanford Sediment may be associated with release due to sudden expansion of swelling clays.

The total amounts of fines released from the Hanford Sediment were in the order of 3-4 mg/g (~0.3 mg/g for the Silica Sand). The large amount of released particles has a potential importance for either change in sediment permeability (clogging of pores due to fines accumulation), or for migration of contaminants with high affinity to the solid phase (rapid transport of fines through the pores). At the Hanford Site naturally borne particles could be detached from the sediment matrix when salinity falls below the CSC due to the dilution of the contaminant plume. These fines may then be transported through the layers of coarse sediments. The relatively high CSC value and the minor particle release observed at salinities above the CSC suggests the presence of mobile particles even at relatively high salt concentrations. This is especially important under the aspect of colloid facilitated contaminant transport. The complex interactions between final salinity, gradient in salinity, hydrodynamic forces, availability and mineralogy of particles on the matrix surfaces all have an impact on particle release and are often difficult to distinguish. The method described here could facilitate a more detailed study of these influences and their relative importance for particle release from sediments as a result of changing salinity.

## 2.7 ACKNOWLEDGEMENTS

We thank Joe Ryan for his thoughtful comments on this manuscript, Reed Glasmann for the analysis of the mineralogical composition of the Hanford

Sediments and Clay Cooper for the particle size analysis. This research was funded by the Department of Energy under contract # DE-FG07-98ER14925 and the Oregon Agricultural Experimental Station.

## 2.8 REFERENCES

- Amrhein C., P.A. Mosher, and J.E. Strong, 1993. **Colloid-Assisted Transport of Trace Metals in Roadside Soils Receiving Deicing Salts.** Soil Sci. Soc. Am. J., 57, 1212-1217.
- Bergendahl, J. & D. Grasso, 1998. **Colloid Generation During Batch Leaching Tests: Mechanics of Disaggregation.** Colloid Surface A, 135, 193-205.
- Cerda, C.M., 1987. **Mobilization of Kaolinite Fines in Porous Media.** Colloid Surface A, 27, 219-241.
- Faure, M.-H., M. Sardin and P. Vitorge, 1996. **Transport of Clay Particles and Radioelements in a Salinity Gradient: Experiments and Simulations.** J. Contam. Hydrol., 21, 255-267.
- Frenkel, H., J.O. Goertzen and J.D. Rhoades, 1978. **Effects of Soil Type and Content, Exchangeable Sodium Percentage, and Electrolyte Concentration on Clay Dispersion and Soil Hydraulic Conductivity.** Soil Sci. Soc. Am. J., 42, 32-39.
- GJPO, 1996. **Vadose Zone Characterization Project at the Hanford Tank Farms.** SX Tank Farm Report. GJ-HAN-DOE/ID12548-268 (GJPO-HAN-4). US Department of Energy, Grand Junction Projects Office, Grand Junction, CO.
- Goldenberg, L.C., M. Magaritz, A.J. Amiel and S. Mandel, 1984. **Changes in hydraulic conductivity of laboratory sand-clay mixtures caused by a seawater-freshwater interface.** J. Hydrol., 70, 329-336.
- Grolimund, D., M. Borkovec, K. Barmettler, and H. Sticher, 1996. **Colloid-Facilitated Transport of Strongly Sorbing Contaminants in Natural Porous Media: A Laboratory Column Study.** Environ. Sci. Technol., 30 (10), 3118-3123.
- Grolimund, D., M. Elimelech, M. Borkovec, K. Barmettler, R. Kretzschmar and H. Sticher, 1998. **Transport of in Situ Mobilized Colloidal Particles in Packed Soil Columns.** Environ. Sci. Technol., 32 (22), 3562-3569.
- Kallay, N., B. Biskup, M. Tomic and E. Matijevic, 1986. **Diffusional Detachment of colloidal Particles from Solid/Solution Interfaces.** Adv. Colloid Interface Sci., 27, 1-42.



- Kallay, N., E. Barouch and E. Matijevic, 1987. **Particle Adhesion and Removal in Model Systems – The Effect of Electrolytes on Particle Detachment.** J. Colloid and Interface Sci., 114, (2), 357-362.
- Kaplan D.I., P.M. Bertsch, D.C. Adriano and W.P. Miller, 1993. **Soil-Borne Mobile Colloids as Influenced by Water Flow and Organic Carbon.** Environ. Sci. Technol., 27 (6), 1193-1200.
- Kaplan, D. I., M.E. Sumner, P.M. Bertsch and D.C. Adriano, 1996. **Chemical Conditions Conducive to the Release of Mobile Colloids from Ultisol Profiles.** Soil Sci. Soc. Am. J., 60, 269-274.
- Kersting, A.B., D.W. Efur, D.L. Finnegan, D.J. Rokop, D.K. Smith and J.L. Thompson, 1999. **Migration of Plutonium in Groundwater at the Nevada Test Site.** Nature, 397, 56-59.
- Khilar, K.C. and H.S. Fogler, 1998. Theory and Applications of Transport in Porous Media, Volume 12: **Migration of Fines in Porous Media.** Kluwer Academic Publishers, Dordrecht, pp 171.
- Khilar, K.C. & H.S. Fogler, 1984. **The Existence of a Critical Salt Concentration for Particle Release.** J. Colloid Interface Sci., 101 (1), 214-224.
- Kia, S.F., H.S. Fogler and M.G. Reed, 1987. **Effect of pH on Colloidally Induced Fines Migration.** J. Colloid Interface Sci., 118, (1), 158-168.
- Kretzschmar, R., M. Borkovec, D. Grolimund and M. Elimelech, 1999. **Mobile Subsurface colloids and their role in contaminant transport.** Adv. Agron., 66, 121-193.
- McCarthy, J.F. and J.M. Zachara, 1989. **Subsurface transport of contaminants.** Environ. Sci. Technol., 23 (5), 496-502.
- Miller, W.P., H. Frenkel and K.D. Newman, 1990. **Flocculation Concentration and Sodium/Calcium Exchange of Kaolinitic Soil Clays.** Soil Sci. Soc. Am. J., 54, 346-351.
- Mohan, K.K., M.G. Reed and H.S. Fogler, 1999. **Formation Damage in Smectite Sandstones by High Ionic Strength Brines.** Colloid Surface A, 154, 249-257.
- Mohan, K.K. and H.S. Fogler, 1997. **Colloidally Induced Smectite Fines Migration: Existence of Mikroquakes.** AIChE J., 43 (3), 565-476.

- Newman, K.A. and K.D. Stolzenbach, 1996. **Kinetics of Aggregation and Disaggregation of Titanium Dioxide Particles and Glass Beads in a Sheared Fluid Suspension.** Colloid Surface A, 107, 189-203.
- Nightingale, H.I. and W.C. Bianchi, 1977. **Groundwater Turbidity Resulting from Artificial Recharge.** Ground Water, 15 (2), 146-152.
- Nocito-Gobel, J. and J.E. Tobiason, 1996. **Effects of Ionic Strength on Colloid Deposition and Release.** Colloid Surface A, 107, 223-231.
- Puls, R.W. and R.M. Powell, 1992. **Transport of Inorganic Colloids Through Natural Aquifer Material: Implications for Contaminant Transport.** Environ. Sci. Technol., 26 (3), 614-621.
- Quirk, J.P. and R.K. Schofield, 1955. **The Effect of Electrolyte Concentration on Soil Permeability.** J. Soil Sci., 6 (2), 163-178.
- Raveendraan, P. and A. Amirtharajah, 1995. **Role of Short-Range Forces in Particle Detachment during Filter Backwashing,** J. Environ. Eng.-ASCE, 121 (12), 860-868.
- Roy, S.B. and D.A. Dzombak, 1996. **Colloid Release and Transport Processes in Natural and Model Porous Media.** Colloid Surface A, 107, 245-262.
- Ryan, J. N., T.H. Illangasekare, M.I. Litaor and R. Shannon, 1998. **Particle and Plutonium Mobilization in Macroporous Soils during Rainfall Simulations.** Environ. Sci. Technol., 32 (4), 476-482.
- Ryan, J.N. and M. Elimelech, 1996. **Review: Colloid Mobilization and Transport in Groundwater.** Colloid Surface A, 107, 1-56.
- Saiers, J.E. and G.M. Hornberger, 1999. **The Influence of Ionic Strength on the Facilitated Transport of Cesium by Kaolinite Colloids.** Water Resour. Res., 35, (6), 1713-1727.
- Schroth, M., S.J. Ahearn, J.S. Selker and J.D. Istok, 1996. **Characterization of Miller Similar Silica Sands for Laboratory Hydrologic Studies.** Soil Sci. Soc. Am. J., 60 (5), 1331-1339.
- Vaidya R.N. and H.S. Fogler, 1990. **Formation Damage due to Colloidally Induced Fines Migration.** Colloid Surface A, 50, 215-229.
- Weisbrod, N., D. Ronen and R. Nativ, 1996. **New Method for Sampling Groundwater Colloids under Natural Gradient Flow Conditions.** Environ. Sci. Technol., 30, 3094-3101.

Weisbrod, N., M. Niemet, M. Rockhold, T. McGinnis, and J.S. Selker, **Infiltration of Saline Solutions into variably saturated porous media**, *submitted*, 2001.

Weisbrod, N., T. McGinnis, M. Niemet, and J.S. Selker, 2000, **Infiltration Mechanisms of Highly Saline Solutions and Possible Implications for the Hanford Site**, EOS Trans. AGU, 81 (48), Fall Meet. Suppl..

Yan, Y.D., M. Borkovec & H. Sticher, 1995. **Deposition and Release of Colloidal Particles in Porous Media**. Prog. Coll. Pol. Sci., 98, 132-135.

### **3 PERMEABILITY CHANGES IN LAYERED HANFORD SEDIMENTS AS A RESULT OF PARTICLE RELEASE**

Theresa Blume, Noam Weisbrod and John S. Selker

*Department of Bioengineering, Oregon State University, Corvallis, OR, 97331*

### 3.1 ABSTRACT

One of the mechanisms of sudden particle release from grain surfaces is a decrease in salt concentration of the permeating fluid down to the critical salt concentration, below which repulsion forces between fine particles and matrix surfaces exceed the forces of attraction. Particle release can cause a change in hydraulic conductivity of the matrix, either by washing out the fines and thus increasing the pore sizes or by plugging of pore constrictions. The phenomenon of permeability changes as a result of particle detachment was investigated in a series of column experiments. Coarse and fine sediments from the Hanford Formation in southeast Washington were tested. Columns were subject to a pulse of highly saline solution ( $\text{NaNO}_3$ ) followed by a freshwater shock causing particle release. Outflow rates and changes in hydraulic head as well as electric conductivity and pH were monitored over time. No permeability decrease occurred within the coarse matrix alone. However, when a thin layer of fine sediment was imbedded within the coarse material (mimicking field conditions at the Hanford Site), permeability decreased down to 10 % of the initial value during the freshwater shock. Evidence suggests that most of this permeability decrease was a result of particles detached within the fine layer and its subsequent clogging. Nevertheless, occlusion due to swelling clays may have also contributed to this permeability reduction. An additional observation was a sudden increase in pH in the outflow solution, generated in-situ during the freshwater shock.

### 3.2 INTRODUCTION

An abrupt change in soil solution or groundwater salinity can cause particle release and subsequent changes in hydraulic conductivity. This phenomenon has been investigated by researchers in several different contexts: in irrigation of soils with sodic waters (*Frenkel et al.* 1978; *Pupisky and Schainberg* 1979; *Shainberg et al.* 1981; *Quirk and Schofield* 1955), at the seawater-freshwater interface in coastal aquifers (*Goldenberg and Magaritz* 1983; *Goldenberg et al.* 1984), and during the process of oil extraction where this phenomenon is called 'water sensitivity' and the resulting decrease in hydraulic conductivity is called 'formation damage' (*Baudracco* 1990; *Khilar and Fogler* 1984; *Khilar et al.* 1983; *Kia et al.* 1987; *Mohan et al.* 1999; *Ochi and Vernoux* 1998; *Vaidya and Fogler* 1990).

Changes in ionic strength may modify the balance between the forces at the particle-grain interface and result in particle detachment (*Cerda* 1987; *Khilar and Fogler* 1998; *Kretzschmar et al.* 1999; *Vaidya and Fogler* 1990). The released particles can then be transported with the permeating solution. As a result permeability can either be increased (by washing out the fines and thus increasing the pore sizes) or decreased (by clogging the pore necks with the fine particles). This is not only of interest in the cases mentioned above but also in the context of contaminant transport. Transport of contaminants with a high affinity for the solid phase has the potential to be enhanced by mobilized fine particles (e.g., *Kersting et al.* 1999; *McCarthy and Zachara* 1989; *Ryan and Elimelech* 1996; *Saiers and*

*Hornberger 1999; Weisbrod et al. 1996*). Increasing or decreasing permeability due to particle release will thus also have an effect on the extent of particle and, consequently contaminant migration, and can be of significant importance at waste storage facilities such as the Hanford Site in southeast Washington. Here, among other sources, single-shelled tanks filled with highly radioactive waste were leaking into the Hanford formation for many years. The leaking waste solution included extremely high concentration of salts ( $> 5 \text{ mol/l Na}^+$ ) as well as radionuclides, other toxic metals, and some organic compounds (*GJPO 1996*). Recently it was shown that the high surface tension of such extremely saline solution might enhance its downward migration (*Weisbrod et al. submitted*). While migrating in the vadose zone, these hyper-saline solutions could be diluted dramatically by both, mixing with the permeating solution or with condensated water vapor osmotically derived from the surrounding sediment (*Weisbrod et al. 2000*). This will result in decreasing ionic strength of the solution and possibly subsequent release of particles. In previous work (see chapter 2) it was shown that a sudden change in salinity resulted in significant particle detachment from coarse Hanford sediments at salt concentrations of  $\sim 0.1 \text{ mol/l NaNO}_3$ .

Thus, mobilization of fines and possible changes in permeability are of specific interest in Hanford sediments. In this study it was attempted to investigate the potential permeability changes in sediments of the Hanford Formation due to changes in solution concentration. The Hanford Formation is distinctively layered with more consolidated fine-grained layers, which are generally thinner, alternating

with more loose coarse layers, which are generally of greater thickness (**Figure 3.1**). As sedimentary basins generally show this characteristic layered pattern, the experiments described in this paper mimic the larger natural system by including a layer of fine sediment imbedded in the coarser sediment in the experimental set-up.



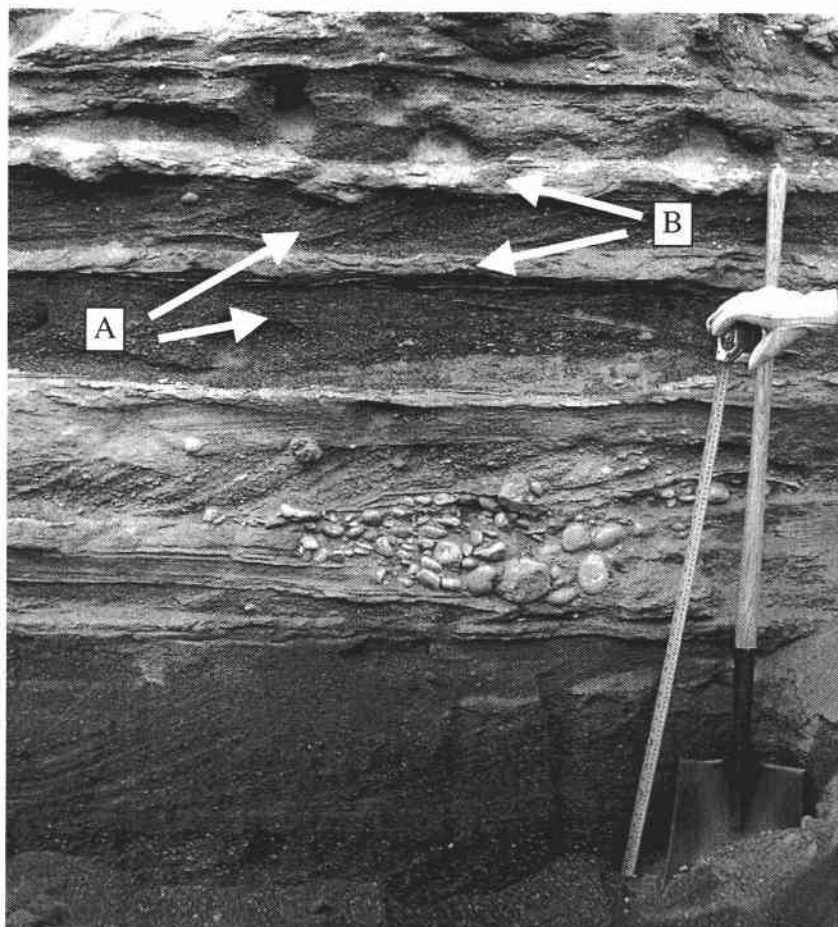


**Figure 3.1** Hanford Formation: layers of coarse (A) and fine (B) sediment. Samples used in this study were obtained 3m below the surface in the 200E Area of the Hanford Site.

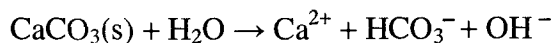
### 3.3 THEORY

According to the modified DLVO theory (Derjaguin-Landau-Verwey-Overbeek) (Khilar and Fogler 1998), particles and matrix are subject to a number of repulsive and attractive forces (e.g. repulsive double layer forces, attractive van der Waals forces, short range Born repulsion forces), the sum of which is the total interaction energy ( $V_T$ ):

$$V_T = V_A + V_R = V_{LVA} + V_{BR} + V_{DLR} \quad (1)$$

where  $V_A$  is the attractive energy (J),  $V_R$  is the repulsive energy (J),  $V_{LVA}$  is the London–van der Waals energy of interaction (J),  $V_{BR}$  is the Born interaction energy (J), and  $V_{DLR}$  is the double-layer energy of interaction (J) (*Khilar and Fogler 1998; Kretzschmar et al. 1999*). High salt concentration results in increasing attraction forces between the matrix and the fine particles attached to its surface. For particles to detach, this higher energy barrier has to be overcome. A decrease in ionic strength results in a decreasing height of this barrier until the critical salt concentration (CSC) is reached, the energy barrier reduces to zero and repulsion forces dominate, causing the attached particles to be released (*Khilar and Fogler 1984; Kretzschmar et al. 1999*).

A change in pH can also prompt or enhance particle release, as the total interaction potential becomes less attractive with increasing pH (*Kia et al. 1987; Vaidya and Fogler 1990*). In Berea Sandstone, for example, the DLVO theory predicts the total interaction potential to become zero at pH 11 for the case of a  $\text{Na}^+$  dominated system (*Vaidya and Fogler 1990*). In-situ changes of pH in natural sediments can be the result of calcite dissolution:



The increasing concentration of  $\text{OH}^-$  in solution is causing an increase in pH. For calcite dissolution in pure water, in a system closed to the atmosphere, this can yield a pH value of 9.95 at the point of equilibration. Ionic strength effects and Calcium complexation are neglected in this calculation (*Snoeyink and Jenkins 1980*).

p 282). Calcite dissolution can be enhanced under conditions of particle release, as fine calcite particles detach from the matrix and their surface area increases. Exchange of  $H^+$  in the solute phase with  $Na^+$  from the matrix is another possible reason for an increase in pH. This is likely to happen during a freshwater shock after percolation of high concentration sodium salt solution (*Kia et al. 1987; Vaidya and Fogler 1990*). Again the relative concentration of  $OH^-$  in solution will increase.

Once released, the particles can either redeposit on the matrix, be transported with the flow, or get entrapped at pore constrictions (**Figure 3.2**). Whether transport or entrapment occurs is dependent on characteristics of the particles, the matrix, and the solution. Important parameters include the pore structure, the size and concentration of the released particles, the flow velocity, and the chemical composition of the liquid phase (*Herzig et al. 1970; Muecke 1979*).

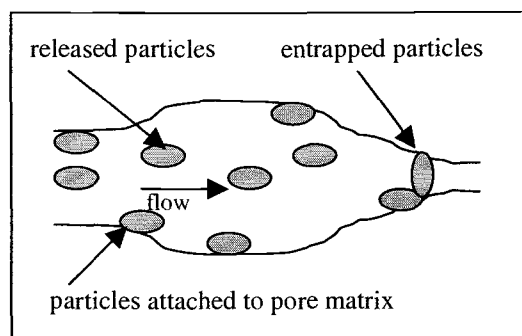


**Figure 3.2** Conceptual diagram of the pore-particle system (after *Khilar and Fogler, 1983*).

*Khilar and Fogler (1998)* distinguished between several different mechanisms of entrapment depending on the ratio of particle size to size of pore constrictions: plugging due to blocking or size exclusion; plugging due to bridging and multiparticle blocking; and a combination of plugging due to surface deposition, bridging and multiparticle blocking.

Other possible causes for permeability reductions are: (1) swelling of clays or (2) swelling induced migration of fine particles. The swelling of clays such as montmorillonite causes a reduction of cross-sectional area of the pore constrictions, which consequently reduces permeability (*Mohan and Fogler 1997*). *Mohan et al. (1999)* attributed part of the permeability reduction observed in Stevens Sandstone to swelling of clays, while the rest of the permeability decrease was attributed to clogging following particle migration. Swelling-induced migration of fines refers to particle displacement as a result of the sudden expansion of clays during a transition in swelling regime from crystalline to osmotic swelling. Crystalline

swelling is a result of the hydration of the cation, while osmotic swelling is usually explained with the expanding double layers of the DLVO theory (see *Mohan and Fogler (1997)* for details). In the crystalline regime the spacing of the clay platelets is increased in discrete increments as water layers are incorporated as a result of decreasing salinity. The transition is marked by a large discrete jump in spacing of clay platelets, after which the separation distance is a continuous function of the salt concentration of the permeating liquid (*Mohan and Fogler. 1997, Mohan et al. 1999*).

Flow through saturated homogeneous porous media at low Reynolds numbers may be described by Darcy's law

$$Q = -KA \frac{H_1 - H_0}{L} \quad (2)$$

where  $Q$  is the flow rate ( $\text{m}^3/\text{s}$ ),  $K$  is the saturated hydraulic conductivity ( $\text{m/s}$ ),  $A$  is the cross-sectional area of the column ( $\text{m}^2$ ),  $H_0$  and  $H_1$  are hydraulic heads ( $\text{m}$ ), and  $L$  ( $\text{m}$ ) is the length of the column. The intrinsic permeability  $k_i$  ( $\text{m}^2$ ), which is a function of the media alone, is computed from the measured hydraulic conductivity and the viscosity and density of the permeating fluid.

$$k_i = K \frac{\mu}{\rho g} \quad (3)$$

where  $K$  is the saturated hydraulic conductivity ( $\text{m/s}$ ),  $\mu$  the dynamic viscosity ( $\text{kg}/(\text{m}\cdot\text{s})$ ),  $\rho$  the density ( $\text{kg}/\text{m}^3$ ) and  $g$  the acceleration of gravity ( $\text{m}/\text{s}^2$ ) (*Fetter 1994, p. 96*).

### 3.4 MATERIALS AND METHODS

#### 3.4.1 Sediments, Glass Beads and Solutions

Three different types of matrix materials were used in this study: (a) natural sediment from a coarse layer of the Hanford Formation (**Figure 3.1**), (b) sediment from the fine layer of the Hanford Formation (**Figure 3.1**) and (c) commercial spherical glass beads # 3000 with a diameter of 1 mm. The Hanford samples used in this study were obtained 3m below the surface in the 200E Area of the Hanford Site, about 1km from the tank farm. The sediment from the Hanford Formation was chosen due to the potential importance of colloidal release from these sediments at the Hanford Site. Only the fraction  $< 2$  mm was used for the experiments. Hereafter the materials from the coarse and fine layers of the Hanford formation will be referred to as 'Coarse Sediment' and 'Fine Sediment'. As it was taken from the site the Coarse Sediment was unconsolidated, while the Fine Sediment layers were consolidated and difficult to break by hand when dry. Glass beads were chosen as an inert matrix for the second set of experiments.  $\text{NaNO}_3$  solution in different concentrations was applied to the column matrix. The maximum concentration was 5 mol/l, and the minimum 0.0004 mol/l. De-ionized water was used for dilution and no buffer was added. All experiments were conducted at regulated room temperature (20-23°C).

Particle size distributions for the released particles were determined by sequential filtration of 10 ml solution through a Millipore® Swinnex-25 filtration

device with Nuclepore® polycarbonate membrane filters with pore sizes of 10, 8, 5, 2, 0.4, 0.1  $\mu\text{m}$ . Absorbance of the remaining solution/particle suspension was measured spectro-photometrically with a Bausch and Lomb® Spectronic 21 at 600 nm after each filtration step to estimate the amount of particles in each size class. A calibration curve was used to convert absorbance values to particle concentration. Size fractionation of the two Hanford Sediments was achieved by sieving and the clay size fraction was determined with the pipette method. This rendered particle size distribution curves for both sediments as well as the uniformity coefficient and  $d_{50}$  values. Particle size analysis was done for three samples for the Coarse and two samples of the Fine Sediment.

Mineralogical composition of the Hanford Sediments was determined with X-ray analysis. Sediment samples were hand ground to fine powder using a diamondite mortar and pestle. The powders were mounted into aluminum sample holders against a glass plate, lightly compressed so as to minimize preferred orientation of platy minerals, then analyzed with a computer-assisted Philips XRD 3100 X-ray Diffractometer utilizing monochromatic Cu  $K\alpha$  radiation (40 kv, 35 ma; quartz reference intensity = 37500 counts/sec). Scans were obtained over an angular 2-theta range of 5-50 degrees with a 0.04 degree step increment and 2 second count time. Digital data were analyzed using Jade 3.1 software. The approximate volume of clay in the suspended fraction was estimated using intensity relations of known clay/quartz/feldspar mixtures. The released fraction of the Hanford sample consisted of fine powder (generally  $<20\text{-}\mu\text{m}$ ) and was analyzed

without further grinding by backloading the powder into aluminum sample holders. Following the initial analysis, the fine powder was re-suspended in distilled water in a 50-ml centrifuge tube, stirred, and allowed to settle for 5 minutes. The suspended portion was decanted into another centrifuge tube and the fines were concentrated by centrifuging for 10 minutes at 10,000 rpm using a Sorval RC-5B refrigerated centrifuge. It is expected that these concentrated fines consist of the  $<5\text{-}\mu\text{m}$  component of the original dispersed particles. A sample of this material was prepared for XRD analysis by smearing the clay onto a glass slide and drying at room temperature. Chemical composition of both sediments was determined by ICP (inductively coupled plasma emission spectroscopy, Perkin and Elmer® Optima 3000). Calcite was determined separately with the 'Approximate Gravimetric Method' (Carter 1993, p.179). A preweighed sediment sample was reacted with 10ml of  $\text{FeCl}_2 \cdot 4\text{H}_2\text{O}$  dissolved in HCl (4mol/l). The weight loss due to released  $\text{CO}_2$  was used to calculate the calcium carbonate content.

#### 3.4.2 Experimental Procedure

Two sets of four column experiments each were run to investigate changes in permeability due to particle release. The column had a cross-sectional area of  $7.55\text{ cm}^2$  and a length of 27 cm. Four ports, spaced 5cm apart along the column were connected to manometers (**Figure 3.3**).



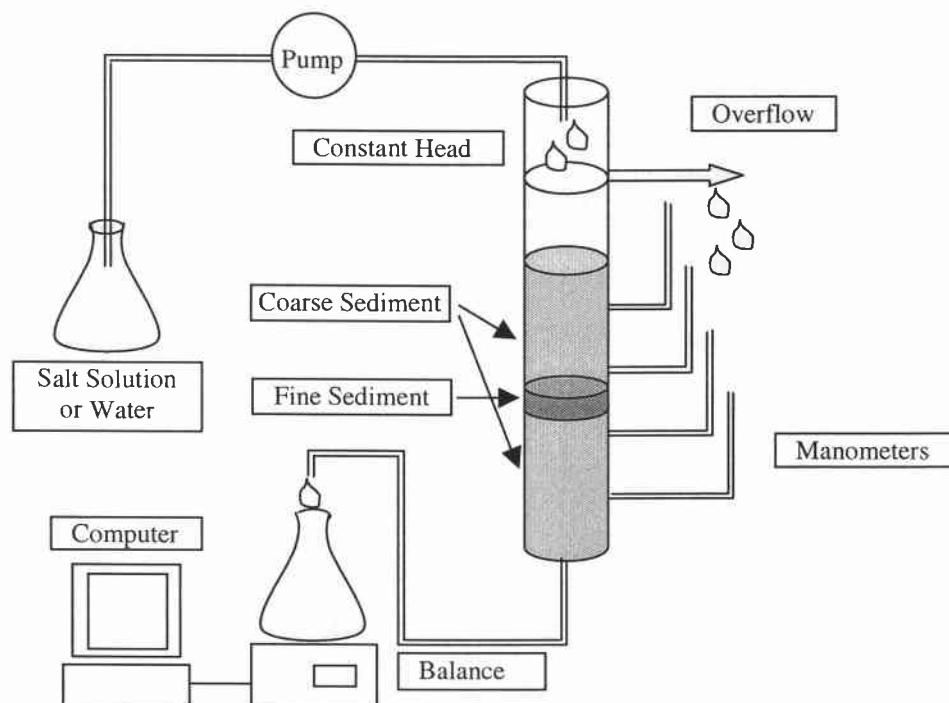


**Figure 3.3** Experimental set-up.

In the first set of experiments the columns were packed with Coarse Sediment to a height of about 20 cm with an on average  $1.2 (\pm 0.3\text{cm})$  cm thick layer of Fine Sediment 10 cm above the outlet. Columns were packed dry, using a randomizing funnel containing three sequential meshes to ensure a homogeneous pack. Next, the column was saturated, first with  $\text{CO}_2$  to prevent entrapment of air, followed by typically at least three pore volumes of  $0.18 - 0.56 \text{ mol/l NaNO}_3$ . This salt concentration, above the CSC, was chosen to prevent particle release during the saturation process. In the second set of experiments the columns were packed with glass beads replacing the coarse Hanford material while the fine layer with an average thickness of  $1.7 \text{ cm} (\pm 0.3 \text{ cm})$  still consisted of Fine Sediments. The

packing procedure was changed to wet packing as the large difference in capillary forces between the Fine Sediment and the glass beads resulted in increasing problems with gas bubble entrapment during saturation. Additionally, an experiment was run where a column was packed with the Coarse Sediment only (without imbedding a layer of Fine Sediment) to determine the effect of particle release on hydraulic conductivity of the Coarse Sediment alone. Constant head conditions were established by ponding solution at a height of 24 cm above column outlet. The height of the pond was defined by the position of the overflow.

After establishing flow at the salinity at which the column was saturated, a minimum of 30 ml of highly concentrated salt solution (5 mol/l) was applied followed by solution of extremely low salinity (0.0002 mol/l), far below the CSC of 0.1 mol/l determined for the Hanford Sediment (see chapter 2). After stabilizing at the reduced permeability, the column was treated with a second salt/freshwater pulse to assess the reversibility of the observed permeability reduction in two of the experiments.

Outflow, in weight over time, was measured continuously and logged in 2-minute intervals. To achieve this frequency of measurements a SETRA balance (Model 5000L) was connected to a computer delivering direct output in an EXCEL spreadsheet format. Heads, pH (determined with pHydrion paperstrips) and electric conductivity (EC) were measured at larger intervals. EC was measured with a GLA® Instant EC Salinity Drop Tester, while heads were measured with the PVC tube manometers described above (**Figure 3.3**).

To investigate the amount of particle release from the Coarse as well as the Fine Sediment, columns were packed with each sediment separately and salt solution (5 M  $\text{NaNO}_3$ ) alternating with de-ionized water was applied in cycles consisting of 3 pore volumes of water and 1 pore volume of salt solution. A pump was used to increase flow through the Fine Sediment, as the permeability was too low to allow reasonably fast flow under a natural head gradient. A flowrate of 1.2 ml/min was established. EC of the outflow was determined as described above, while particle concentration was determined by light absorption, measured spectrophotometrically with a Bausch and Lomb® Spectronic 21 at 600 nm and converted to particle concentration using a calibration curve. The particles released during these experiments were then used to analyze particle size distribution with the procedure described in section 3.4.1.

## 3.5 RESULTS

### 3.5.1 Sediment Properties

The mineralogy of Coarse Sediment is dominated by anorthitic plagioclase and ferromagnesian minerals common to basalt (augite and hornblend). Quartz is a relatively minor component of the Hanford Sediment, reflecting the absence of this mineral in basalt. Clay minerals are only a trace component and include mica (biotite and muscovite). In general, the clay content is <10% in the Coarse Sediment and probably represents undispersed mud fragments or cemented soil clasts. The Fine Sediment is less enriched in basaltic rock fragments relative to the

Coarse Sediment and sample mineralogy was enriched in quartz, mica, and K-feldspar relative to the basaltic coarse sand fraction. The increased abundance of granitic components (quartz, K-feldspar, mica) in the Fine Sediment reflects concentration of upper Columbia River sourced sediments in this sample, although the basaltic components of augite, Ca-plagioclase, and amphibole are also present. Mica, smectite, and chlorite/kaolinite are common minor components of the Fine Sediment, which has a total clay content of about 20-25%. This can include silt and sand-sized mica.

The released particles of the Hanford Sediment consist of a mixture of clay and non-clay minerals. The clay mineral assemblage includes smectite (montmorillonite), mica (most likely muscovite and biotite), chlorite, and kaolinite. Mica appears to dominate the clay assemblage of both all fractions, but smectite is generally enriched in the finer sediment concentrate. Clay minerals compose about 40-50% of the detached particles, although clays are more abundant in the  $<5\text{-}\mu\text{m}$  fraction (60-70%). The non-clay fraction includes quartz, Ca-rich plagioclase, augite, hornblende, traces of K-feldspar, and iron oxides. Quartz abundance exceeds that of plagioclase and may represent glacial silt derived from the upper Columbia River basin during episodic glacial outburst floods. The calcite content of the Fine Sediment determined with the approximate gravimetric method ranged at 0.5 %.

The  $d_{50}$  of the Coarse Sediment was 0.67 mm and 0.07 mm for the Fine Sediment with a large silt fraction (35-52 %). The uniformity coefficient ( $d_{60}/d_{10}$ )

of the Fine Sediment (4.92) is higher than for the Coarse Sediment (3.03) as it contains a large fraction of fines combined with a small coarse fraction. Grain size distribution curves for both the Coarse and the Fine Sediment are shown in **Figure 3.4**. The cation exchange capacity (CEC) for the Fine Sediment is more than twice as high than for the Coarse Sediment (**Table 1**).

**Table 3.1** Chemical analyses and physical properties of the sediments.

Sediment	K ppm	Ca meq/ 100g	Mg meq/ 100g	Na meq/ 100g	Mn ppm	Fe ppm	d <sub>60</sub> /d <sub>10</sub>	d <sub>50</sub> mm	CEC meq/ 100g
<b>Hanford Fine</b>	222	12.4	2.7	1.29	0.5	5.0	4.92	0.07	9.7
<b>Hanford Coarse</b>	121	4.9	1.4	0.63	0.4	4.6	3.03	0.67	4.1

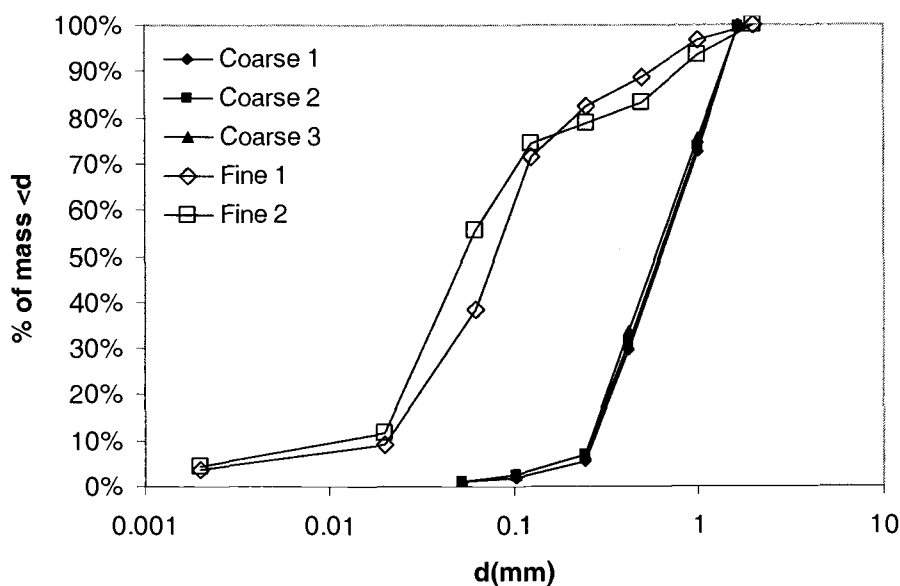


**Figure 3.4** Grain size distribution curves for three samples of the Coarse and the two samples of the Fine Sediment.

The hydraulic conductivity of the Coarse Sediment was determined using Darcy's law and then converted to intrinsic permeability using equation (3). It was on the order of  $0.014 \text{ cm}^2$  with a standard deviation of  $0.003 \text{ cm}^2$ . The glass beads had an intrinsic permeability of  $0.52 \text{ cm}^2$  ( $0.01 \text{ cm}^2$  standard deviation). For the Fine Sediment intrinsic permeabilities were calculated from the intrinsic permeability of the 5 cm column section that contained the fine layer. These values ranged from  $0.0004$  to  $0.0025 \text{ cm}^2$ . The high variance in results is probably due to variability in packing of the columns as a consequence of the natural heterogeneity of the Fine Sediment.

### 3.5.2 Particle Release and Changes in Permeability

Particle release from the Fine as well as the Coarse Sediment was a function of salinity. The Fine Sediment released more particles in the 2-5  $\mu\text{m}$  size class (78% compared to 66% in the Coarse Sediment), while more particles were released from the Coarse Sediment in both the  $> 5 \mu\text{m}$  and  $< 2 \mu\text{m}$  size classes (**Figure 3.5**). Note that the sequential filtration process was only run once for each sediment (no repetitions), which means that these size fractionations are to be taken as indicative rather than precise results.

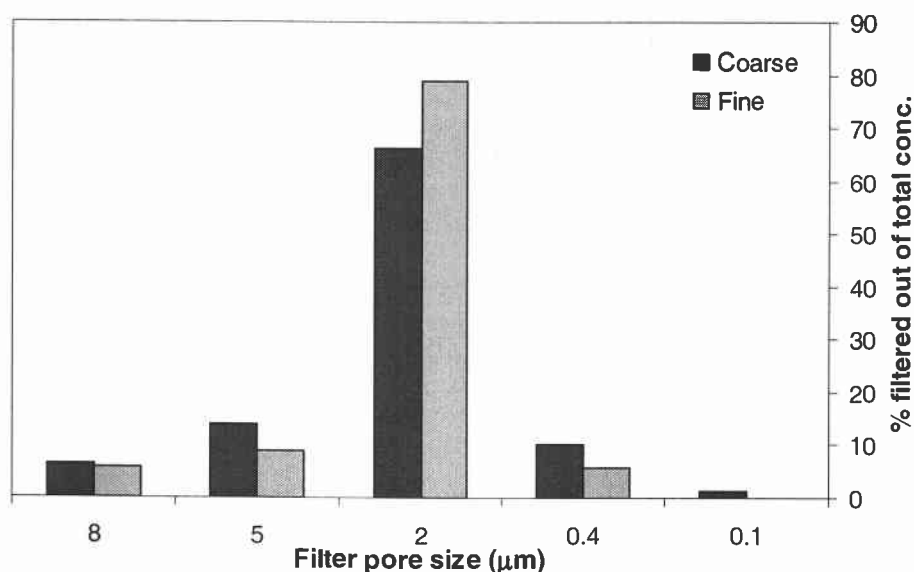


**Figure 3.5** Particle size distribution of released particles from the Coarse and the Fine Sediment. Each column signifies the percentage of particles captured in the filter with the respective pore size (i.e. the 2  $\mu\text{m}$  filter will contain the size fraction from 2 to 5  $\mu\text{m}$ ).

Particle release in columns packed with only Coarse Sediment had a slightly positive effect on intrinsic permeability as an increase was observed from 0.067 to 0.077 cm<sup>2</sup>. Column experiments including a layer of Fine Sediment showed that in this case overall intrinsic permeabilities decreased by 83 to 93 percent during the freshwater shock (**Table 3.2, Experiments 1-3**). The range in reductions is due to variability in column packing.

**Table 3.2** Initial and final values of overall intrinsic permeabilities (cm<sup>2</sup>) of 6 experiments. A layer of Fine Sediment was imbedded either in Coarse Sediment or in glass beads.

Coarse Matrix	Experiment #	k <sub>i0</sub> (initial)	k <sub>iF</sub> (final)	k <sub>iF</sub> /k <sub>i0</sub>
Coarse Sediment	1	0.013	0.0009	0.07
Coarse Sediment	2	0.015	0.003	0.17
Coarse Sediment	3	0.023	0.002	0.09
Glass beads	4	0.005	0.0017	0.31
Glass beads	5	0.004	0.0007	0.20
Glass beads	6	0.0013	0.00017	0.13

To investigate if particles generated within the coarse layer are the cause of clogging, the Coarse Sediment was replaced with glass beads. These glass beads



are assumed to be inert with a clean, particle-free surface. Therefore, all changes in permeability are likely to be due to internal processes within the fine layer. The experiments showed that a significant decrease in hydraulic conductivity occurred even when using the glass bead media. In this case intrinsic permeability was reduced by 69 to 87 percent. Final conductivities were only slightly higher than in the columns containing the Coarse Sediment. On average, the final permeability in the experiments including the Coarse Sediment was 11 % of the initial  $k_i$  ( $\pm 5$  %) while for the glass beads it was 21 % ( $\pm 10$  %) (**Table 3.2, Experiments 4-6**). An example for permeability reduction for each set of experiments can be seen in **Figure 3.6**.

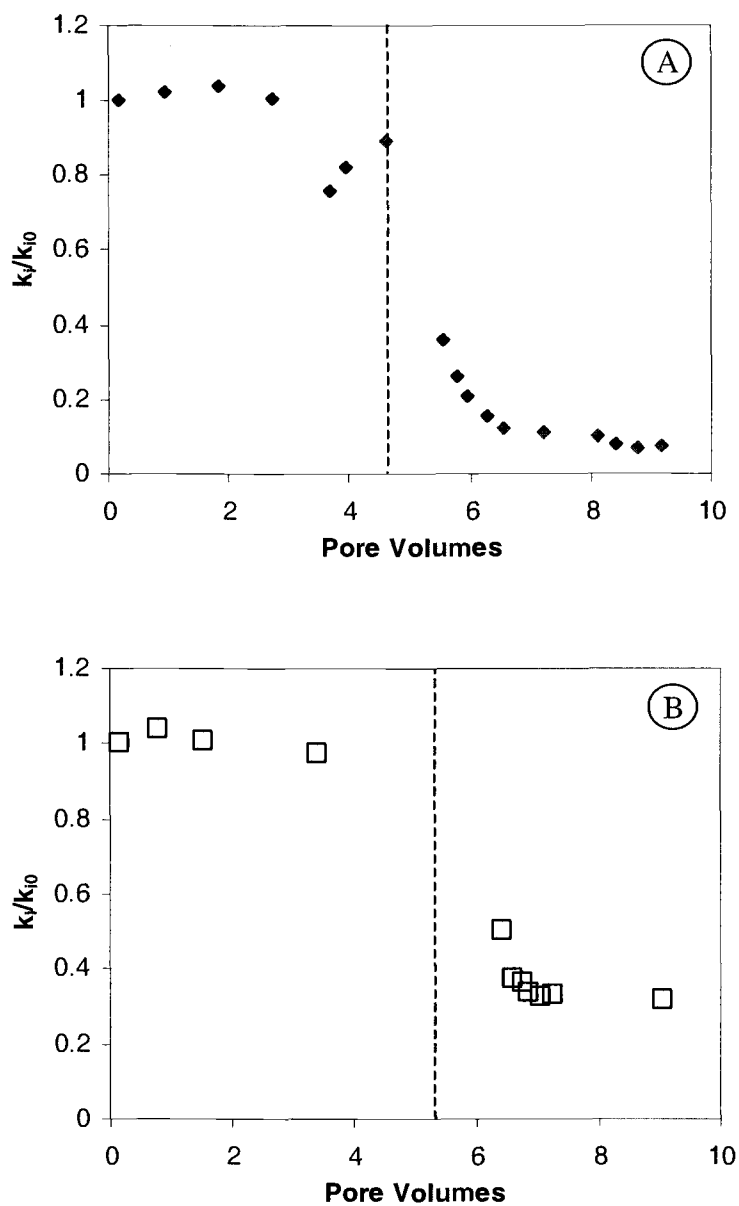


**Figure 3.6** Permeability reduction during a freshwater shock. Shown is one example for both sets of experiments: A Coarse Sediment (experiment #1), B Glass beads (experiment #4). The dashed line marks the change to freshwater. Note that the decrease in case A just prior to the freshwater shock is an artifact due to variations in head as the solutions are exchanged.

The overall  $k_i$  of the packed column decreased simultaneously to the  $k_i$  of the fine layer segment. Overall  $k_i$  values (assuming no permeability changes outside of the fine layer) can be calculated with the following equation

$$k_i(overall) = \frac{x}{\sum \frac{x_i}{k_{ii}}} \quad (5)$$

where  $k_i$  is the intrinsic permeability ( $\text{m}^2$ ),  $k_{ii}$  is the intrinsic permeability ( $\text{m}^2$ ) of the column segments,  $x$  (m) is the overall length of the packed column and  $x_i$  (m) is the length of the column segments (*Fetter 1994*). The calculated values, which attribute all reductions to those measured in the fine layer, fit the data well, showing that the system permeability variations are indeed dominated by the fine layer (**Figure 3.7**).

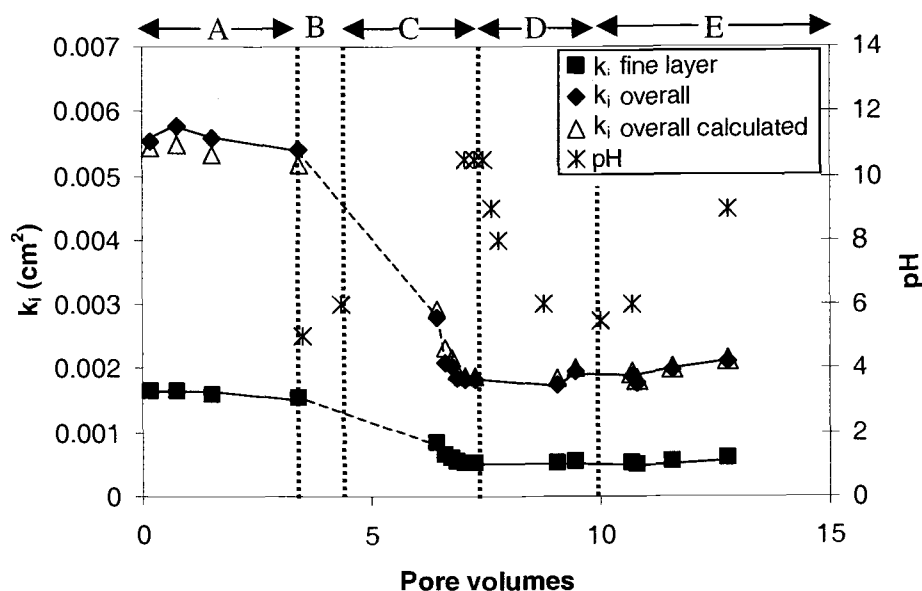


**Figure 3.7** Permeability reduction (overall and in the fine layer segment), and pH changes as a result of freshwater shock (glass bead experiment). The lines signify changes in applied solution. A: salt solution (0.2 mol/l  $\text{NaNO}_3$ ); B: first salt pulse (5 mol/l  $\text{NaNO}_3$ ); C: first freshwater shock (0.0001 mol/l  $\text{NaNO}_3$ ); D: second salt pulse (5 mol/l, then 0.2 mol/l, followed by 5 mol/l  $\text{NaNO}_3$ ); E: second freshwater shock (0.0001 mol/l  $\text{NaNO}_3$ ).

Swelling of montmorillonite as well as particle entrapment are both possible mechanisms for this decrease in permeability. To assess the reversibility of the observed permeability reduction process the column was subsequently treated with a second salt/freshwater pulse. Permeability reduction was irreversible, as the re-application of salt had no observable effect on permeability. The following second freshwater pulse also had no further impact (**Figure 3.7**). If the permeability reduction was caused mainly by swelling, changing back to the original solution should generally reverse the process (Mohan *et al.* 1993; McNeal and Coleman

1966). This and the fact that particle release from the Fine Sediment is extensive (**Figure 3.8**) suggests migrating particles as the major cause of reduced hydraulic conductivity.

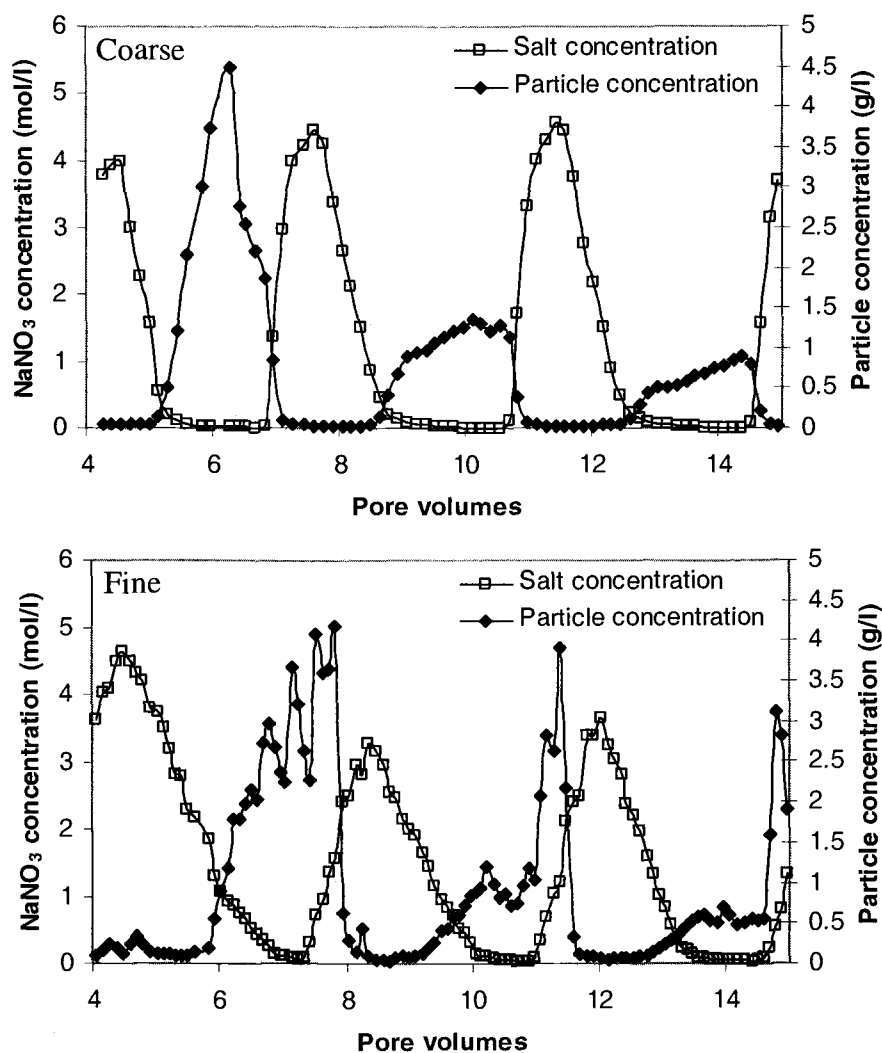


**Figure 3.8** Particle release from both sediments as a function of salinity. Shown here are 3 cycles, each of which consisted of 1 pore volume of 5 M NaNO<sub>3</sub> and 3 pore volumes of de-ionized water. Note that release from the Fine and Coarse Sediment are of the same order of magnitude. In both cases a decrease in salt concentration resulted in particle release.

A sudden increase in pH values from 5 to 10 was observed during the freshwater pulse. **Figure 3.9** shows one of the glass bead experiments, which

demonstrates clearly the coupled phenomena of salinity, pH and permeability change. The pH increase is likely to induce additional reduction permeability. pH changes can be caused for example by dissolution of calcite or exchange of  $H^+$  ions from solution to matrix (see section 3.3). In this case both mechanisms are possible as calcite contents and CEC of the Fine Sediment is relatively high.

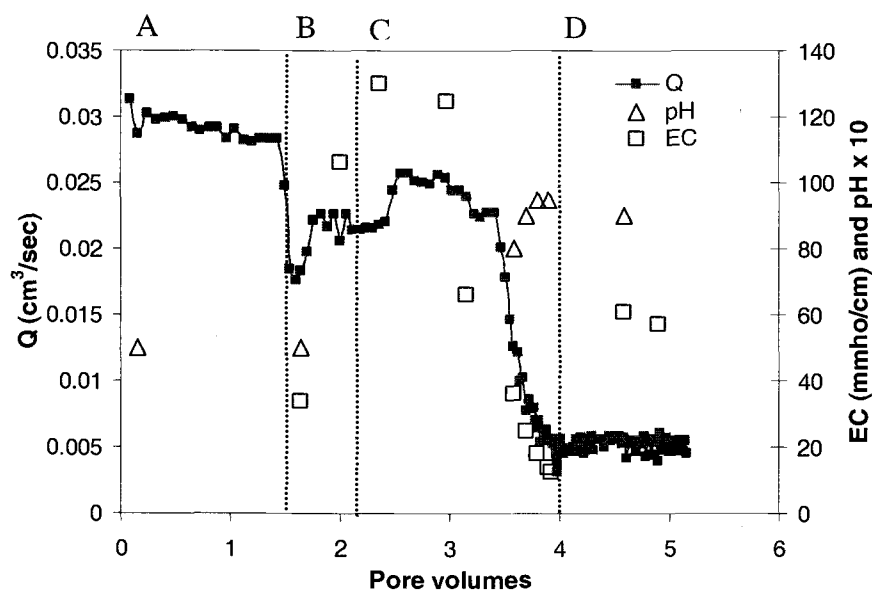


**Figure 3.9** Outflow  $Q$ , EC and pH during a freshwater shock experiment. Shown here is one of the experiments with glass beads. The lines signify changes in applied solution. A: salt solution (0.2 mol/l  $NaNO_3$ ), B: salt pulse (5 mol/l  $NaNO_3$ ); C: freshwater shock (0.0001 mol/l  $NaNO_3$ ); D: second salt pulse (5 mol/l, then 0.2 mol/l  $NaNO_3$ ). The drop in flow rate ( $Q$ ) (which is equivalent to a drop in  $K_{(overall)}$ ) in sections B and C is due to a drop in ponding height when solutions were exchanged.

As the increase of pH in our study was sudden and coupled to the freshwater shock it is likely to be due to cation exchange as well as possibly enhanced dissolution of released calcite particles. A rough calculation of maximal possible impact shows that the fine layer with a CEC of 9.7 meq/100g (Table 1) has the potential of generating 14.5 l of pH 10 solution, if all surface sites were filled with  $\text{Na}^+$  during the salt pulse and if the freshwater shock subsequently replaced all these ions with  $\text{H}^+$ , leaving excess  $\text{OH}^-$  in solution.

### 3.6 SUMMARY AND CONCLUSIONS

A sequence of coarse and fine sediments of the Hanford Formation conditioned with  $\text{Na}^+$  solutions and then subject to a freshwater shock showed significant decrease in hydraulic conductivity. This permeability decrease appears to be the result of detachment of fines from the sediments. Changes in salinity as well as in-situ pH changes increase the repulsion forces within the particle-matrix system, thus causing particle release. In the case of the coarse and fine Hanford sediments, most of the permeability reduction was found to be caused by release and deposition processes within the fine layer. The fact that montmorillonite is present is likely to enhance permeability reduction, either by causing particle release due to sudden expansion or simply by reduction of cross-sectional area of the pore constrictions as swelling increases with lower salinities. Particle detachment or swelling of clays did not cause a reduction in hydraulic conductivity in the Coarse Sediment alone. Since layered systems are common in natural settings, our results



suggest that layers of fine sediment can have a significant effect on the overall permeability changes in the vadose zone in case of particle mobilization. Rather than assuming homogeneously mixed conditions, layered sediments should thus especially be taken into account in studies of permeability changes and colloidally enhanced contaminant transport. For the case of the Hanford Site this could indicate that while vertical flow is inhibited, lateral flow and subsequently lateral contaminant transport is enhanced.

### 3.7 ACKNOWLEDGEMENTS

We thank Reed Glasmann for the analysis of the mineralogical composition of the Hanford Sediments and Clay Cooper for the particle size analysis. This research was funded by the Department of Energy under contract # DE-FG07-98ER14925 and the Oregon Agricultural Experimental Station.

### 3.8 REFERENCES

- Baudracco, J., 1990. **Variations In Permeability and Fine Particle Migrations in Unconsolidated Sandstones Submitted to Saline Circulations.** *Geothermics*, 19 (2), 213-221.
- Carter, M. (Ed.), 1993. **Soil Sampling and Methods of Analysis.** Lewis Publishers, Boca Raton, pp. 823.
- Cerda, C.M., 1987. **Mobilization of Kaolinite Fines in Porous Media.** *Colloid Surface A*, 27, 219-241.
- Fetter C.W., 1994. **Applied Hydrogeology.** Third Edition, Prentice Hall, Upper Saddle River NJ, pp.691.
- Frenkel, H., J.O. Goertzen and J.D. Rhoades, 1978. **Effects of Soil Type and Content, Exchangeable Sodium Percentage, and Electrolyte Concentration on Clay Dispersion and Soil Hydraulic Conductivity.** *Soil Sci. Soc. Am. J.*, 42, 32-39.
- GJPO, 1996. **Vadose Zone Characterization Project at the Hanford Tank Farms.** SX Tank Farm Report. GJ-HAN-DOE/ID12548-268 (GJPO-HAN-4). US Department of Energy, Grand Junction Projects Office, Grand Junction, CO.
- Goldenberg, L.C., M. Magaritz, A.J. Amiel and S. Mandel, 1984. **Changes in hydraulic conductivity of laboratory sand-clay mixtures caused by a seawater-freshwater interface.** *J. Hydrol.*, 70, 329-336.
- Goldenberg, L.C. and M. Magaritz, 1983. **Experimental investigation on irreversible changes of hydraulic conductivity on the seawater-freshwater interface on coastal aquifers.** *Water Resour. Res.*, 19 (1), 77-85.
- Herzig, J.P., D.M. Leclerc and P. Le Goff, 1970. **Flow of Suspensions through Porous Media – Application to Deep Filtration.** *Ind. Eng. Chem.*, 62 (5), 8-35.
- Kersting, A.B., D.W. Efurud, D.L. Finnegan, D.J. Rokop, D.K. Smith and J.L. Thompson, 1999. **Migration of Plutonium in Groundwater at the Nevada Test Site.** *Nature*, 397, 56-59.
- Khilar, K.C. and H.S. Fogler, 1998. **Theory and Applications of Transport in Porous Media, Volume 12: Migration of Fines in Porous Media.** Kluwer Academic Publishers, Dordrecht, pp. 171.

- Khilar, K.C. and H.S. Fogler, 1984. **The Existence of a Critical Salt Concentration for Particle Release.** J. Colloid Interface Sci., 101 (1), 214-224.
- Khilar K.C., H.S. Fogler and J.S. Ahluwalia, 1983. **Sandstone Water Sensitivity: Existence of a Critical Rate of Salinity Decrease for Particle Capture.** Chem. Eng. Sci., 38 ( 5), 789-800.
- Kia, S.F., H.S. Fogler and M.G. Reed, 1987. **Effect of pH on Colloidally Induced Fines Migration.** J. Colloid Interface Sci., 118 (1), 158-168.
- Kretzschmar, R., M. Borkovec, D. Grolimund and M. Elimelech, 1999. **Mobile Subsurface colloids and their role in contaminant transport.** Adv. Agron., 66, 121-193.
- McCarthy, J.F. and J.M. Zachara, 1989. **Subsurface transport of contaminants.** Environ. Sci. Technol., 23 (5), 496-502.
- McNeal, B.L. and N.T. Coleman, 1966. **Effect of Solution Composition on Soil Hydraulic Conductivity.** Soil Sci. Soc. Am. J., 30, 308-312.
- Mohan, K.K., M.G. Reed and H.S. Fogler, 1999. **Formation Damage in Smectite Sandstones by High Ionic Strength Brines.** Colloid Surface A. 154, 249-257.
- Mohan, K.K. and H.S. Fogler, 1997. **Colloidally Induced Smectite Fines Migration: Existence of Mikroquakes.** AIChE J., 43 (3), 565-476.
- Mohan, K.K., R.N. Vaidya, M.G. Reed and H.S. Fogler, 1993. **Water Sensitivity of Sandstones containing Swelling and Non-Swelling Clays.** Colloid Surface A, 73, 237-254.
- Muecke, T.W., 1979. **Formation Fines and Factors Controlling Their Movement in Porous Media.** J. Petrol. Technol., 31, 144-150.
- Ochi, J. & J.-F. Vernoux, 1998. **Permeability Decrease in Sandstone reservoirs by Fluid Injection – Hydrodynamic and Chemical Effects.** J. Hydrol., 208, 237-248.
- Pupisky, H. and I. Shainberg, 1979. **Salt Effects on the Hydraulic Conductivity of a Sandy Soil.** Soil Sci. Soc. Am. J., 43 (3), 429-433.
- Quirk, J.P. and R.K. Schofield, 1955. **The Effect of Electrolyte Concentration on Soil Permeability.** J. Soil Sci., 6 (2), 163-178.

- Ryan, J.N. and M. Elimelech, 1996. **Review: Colloid Mobilization and Transport in Groundwater.** Colloid Surface A, 107,1-56.
- Saiers, J.E. and G.M. Hornberger, 1999. **The Influence of Ionic Strength on the Facilitated Transport of Cesium by Kaolinite Colloids.** Water Resour. Res., 35 (6), 1713-1727.
- Shainberg, I., J.D. Rhoades, and R.J. Prather, 1981. **Effect of Low Electrolyte Concentration on Clay Dispersion and Hydraulic Conductivity of a Sodic Soil.** Soil Sci. Soc. Am. J., 45, 273-277.
- Snoeyink, V.L. and D. Jenkins, 1980. **Water Chemistry.** John Wiley and Sons, New York, pp 463.
- Vaidya R.N. and H.S. Fogler, 1990. **Formation Damage due to Colloidally Induced Fines Migration.** Colloid Surface, 50, 215-229.
- Weisbrod, N., D. Ronen and R. Nativ, 1996. **New Method for Sampling Groundwater Colloids under Natural Gradient Flow Conditions.** Environ. Sci. Technol., 30, 3094-3101.
- Weisbrod, N., M. Niemet, M. Rockhold, T. McGinnis, and J.S. Selker, **Infiltration of Saline Solutions into variably saturated porous media, submitted, 2001.**
- Weisbrod, N., T. McGinnis, M. Niemet, and J.S. Selker, 2000. **Infiltration Mechanisms of Highly Saline Solutions and Possible Implications for the Hanford Site,** EOS Trans. AGU, 81 (48), Fall Meet. Suppl..

## 4 SUMMARY AND CONCLUSIONS

Two aspects of particle release from sediment were studied: (1) at what salt concentration does particle release occur and how can this salt concentration be determined; and (2) does particle release have an effect on sediment permeability?

The three methods described in chapter 2 provided similar CSC values for each sediment, suggesting that batch experiments, especially method 2, are a viable alternative to column-based methods. The advantages of batch experiments include cheaper and simpler experimental set-up, faster repetitions, and greater control of experimental conditions. The plateau seen in case of the batch experiments with the Hanford Sediment would require further investigation to be conclusively explained; however, it is likely the result of the mineralogically heterogeneous nature of both the sediments and the attached particles. Additionally, our findings suggest that CSC values in natural sediments are also influenced by the mineralogical heterogeneity of sediments and fines and the presence of swelling clays. This can lead to high CSC values as observed in the case of the Hanford Sediment.

The total amounts of fines released from the Hanford Sediment were in the order of 3-4mg/g (~0.6mg/g for the Silica Sand). This large amount of released particles has a potential importance for either change in sediment permeability (clogging of pores due to fines accumulation), or for migration of contaminants with high affinity to the solid phase (rapid transport of fines through the pores). At

the Hanford Site naturally borne particles could detach from the sediment matrix when salinity falls below the CSC due to the dilution of the contaminant plume. These fines may then be transported through the layers of coarse sediments. The relatively high CSC value and the minor particle release observed at salinities above the CSC suggests the presence of mobile particles even at relatively high salt concentrations. This is especially important under the aspect of colloid facilitated contaminant transport. The complex interactions between final salinity, gradient in salinity, hydrodynamic forces, availability and mineralogy of particles on the matrix surfaces all have an impact on particle release and are often difficult to distinguish. The method described here could facilitate a more detailed study of these influences and their relative importance for particle release from sediments as a result of changing salinity.

Potential changes in permeability were investigated with column experiments as described in chapter 3. A sequence of coarse and fine sediments of the Hanford Formation subject to a freshwater shock showed significant decrease in hydraulic conductivity. This permeability decrease appears to be the result of detachment of fines from the sediments. Changes in salinity as well as in-situ pH changes increase the repulsion forces within the particle-matrix system, thus causing particle release. In the case of the coarse and fine Hanford sediments, most of the permeability reduction was found to be caused by release and deposition processes within the fine layer. The fact that montmorillonite is present is likely to enhance permeability reduction, either by causing particle release due to sudden expansion

or simply by reduction of cross-sectional area of the pore constrictions as swelling increases with lower salinities. Particle detachment or swelling of clays did not cause a reduction in hydraulic conductivity in the Coarse Sediment alone. Since layered systems are common in natural settings, our results suggest that layers of fine sediment can have a significant effect on the overall permeability changes in the vadose zone and increasing the effective anisotropy of the formation. Rather than assuming homogeneously mixed conditions, layered sediments should thus especially be taken into account in studies of permeability changes and colloidally enhanced contaminant transport. For the case of the Hanford Site this could indicate that while vertical flow is inhibited, lateral flow as well as lateral contaminant transport is enhanced.

## 5 BIBLIOGRAPHY

- Amirtharajah, A. and P. Raveendran, 1993. **Detachment of Colloids from Sediments and Sand Grains.** *Colloid Surface A*, 73, 211-227.
- Amrhein C., P.A. Mosher, and J.E. Strong, 1993. **Colloid-Assisted Transport of Trace Metals in Roadside Soils Receiving Deicing Salts.** *Soil Sci. Soc. Am. J.*, 57, 1212-1217.
- Bates, J.K., J.P. Bradley, A. Teetsov, C.R Bradley, and M. Buchholtz ten Brink, 1992. **Colloid Formation During Waste Form Reaction: Implications for Nuclear Waste Disposal.** *Science*, 256, 649-651.
- Baudracco, J., 1990. **Variations In Permeability and Fine Particle Migrations in Unconsolidated Sandstones Submitted to Saline Circulations.** *Geothermics*, 19 (2), 213-221.
- Bergendahl, J. and D. Grasso, 1998. **Colloid Generation During Batch Leaching Tests: Mechanics of Disaggregation.** *Colloid Surface A*, 135, 193-205.
- Buffle, J. and H.P. van Leeuwen (Eds), 1993. **Environmental Particles.** Lewis Publishers, Boca Banton, Chapter 6, pp 426.
- Carter, M. (Ed.), 1993. **Soil Sampling and Methods of Analysis.** Lewis Publishers, Boca Raton, pp. 823.
- Cerda, C.M., 1987. **Mobilization of Kaolinite Fines in Porous Media.** *Colloid Surface A*, 27, 219-241.
- Degueldre, C., B. Baeyens , W.Goerlich, J. Riga, J. Verbist, and P. Stadelmann, 1989. **Colloids in Water from a Subsurface Fracture in Granitic Rock, Grimsel Test Site, Switzerland.** *Geochim. Cosmochim. Ac.*, 53, 603-610.
- Derjaguin, B.V., and L. Landau, 1941. **A Theory of Stability of Strongly Charged Lyophobic Sols and the Coalescence of Strongly Charged Particles in Electrolytic Solutions.** *Acta Phys.-Chim. USSR*, 14, 633.
- Elimelech, M., J. Gregory, X Jia, and R.A. Williams, 1998. **Particle Deposition and Aggregation.** Butterworth-Heinemann, Woburn, pp 441.
- Everett, D.H., 1988. **Basic Principles of Colloid Science.** Royal Society of Chemistry Paperbacks, London, pp 243.



- Faure, M.-H., M. Sardin and P. Vitorge, 1996. **Transport of Clay Particles and Radioelements in a Salinity Gradient: Experiments and Simulations.** J. Contam. Hydrol., 21, 255-267.
- Fetter C.W., 1994. **Applied Hydrogeology.** Third Edition, Prentice Hall, Upper Saddle River NJ, pp.691.
- Frenkel, H., J.O. Goertzen and J.D. Rhoades, 1978. **Effects of Soil Type and Content, Exchangeable Sodium Percentage, and Electrolyte Concentration on Clay Dispersion and Soil Hydraulic Conductivity.** Soil Sci. Soc. Am. J., 42, 32-39.
- GJPO, 1996. **Vadose Zone Characterization Project at the Hanford Tank Farms.** SX Tank Farm Report. GJ-HAN-DOE/ID12548-268 (GJPO-HAN-4). US Department of Energy, Grand Junction Projects Office, Grand Junction, CO.
- Goldenberg, L.C. and M. Magaritz, 1983. **Experimental investigation on irreversible changes of hydraulic conductivity on the seawater-freshwater interface on coastal aquifers.** Water Resour. Res., 19 (1), 77-85.
- Goldenberg, L.C., M. Magaritz, A.J. Amiel and S. Mandel, 1984. **Changes in hydraulic conductivity of laboratory sand-clay mixtures caused by a seawater-freshwater interface.** J. Hydrol., 70, 329-336.
- Grolimund, D., and M. Borkovec, 1999. **Long-Term Release Kinetics of Colloidal Particles from Natural Porous Media.** Environ. Sci. Technol., 33, (22), 4054-4060.
- Grolimund, D., M. Borkovec, K. Barmettler, and H. Sticher, 1996. **Colloid-Facilitated Transport of Strongly Sorbing Contaminants in Natural Porous Media: A Laboratory Column Study.** Environ. Sci. Technol., 30 (10), 3118-3123.
- Grolimund, D., M. Elimelech, M. Borkovec, K. Barmettler, R. Kretzschmar and H. Sticher, 1998. **Transport of in Situ Mobilized Colloidal Particles in Packed Soil Columns.** Environ. Sci. Technol., 32 (22), 3562-3569.
- Hedges, E. S., 1931. **'Colloids'**, Edward Arnold, London.
- Herzig, J.P., D.M. Leclerc and P. Le Goff, 1970. **Flow of Suspensions through Porous Media – Application to Deep Filtration.** Ind. Eng. Chem., 62 (5), 8-35.

- Kallay, N., B. Biskup, M. Tomic and E. Matijevic, 1986. **Diffusional Detachment of colloidal Particles from Solid/Solution Interfaces.** Adv. Colloid Interface Sci., 27, 1-42.
- Kallay, N., E. Barouch and E. Matijevic, 1987. **Particle Adhesion and Removal in Model Systems – The Effect of Electrolytes on Particle Detachment.** J. Colloid and Interface Sci., 114, (2), 357-362.
- Kaplan D.I., P.M. Bertsch, D.C. Adriano and W.P. Miller, 1993. **Soil-Borne Mobile Colloids as Influenced by Water Flow and Organic Carbon.** Environ. Sci. Technol., 27 (6), 1193-1200.
- Kaplan, D.I., M.E. Sumner, P.M. Bertsch and D.C. Adriano, 1996. **Chemical Conditions Conducive to the Release of Mobile Colloids from Ultisol Profiles.** Soil Sci. Soc. Am. J., 60, 269-274.
- Kersting, A.B., D.W. Efur, D.L. Finnegan, D.J. Rokop, D.K. Smith and J.L. Thompson, 1999. **Migration of Plutonium in Groundwater at the Nevada Test Site.** Nature, 397, 56-59.
- Khilar, K.C. and H.S. Fogler, 1998. Theory and Applications of Transport in Porous Media, Volume 12: **Migration of Fines in Porous Media.** Kluwer Academic Publishers, Dordrecht, pp 171.
- Khilar, K.C. & H.S. Fogler, 1984. **The Existence of a Critical Salt Concentration for Particle Release.** J. Colloid Interface Sci., 101 (1), 214-224.
- Khilar K.C., H.S. Fogler and J.S. Ahluwalia, 1983. **Sandstone Water Sensitivity: Existence of a Critical Rate of Salinity Decrease for Particle Capture.** Chem. Eng. Sci., 38 ( 5), 789-800.
- Kia, S. F., H.S. Fogler, and M.G. Reed, 1987. **Effect of pH on Colloidally Induced Fines Migration.** J. Colloid Interface Sci., 118, (1), 158-168.
- Kretzschmar, R., M. Borkovec, D. Grolimund and M. Elimelech, 1999. **Mobile Subsurface Colloids and their Role in Contaminant Transport.** Adv. Agron., 66, 121-193.
- Liang, L. J.F. McCarthy, L.W. Jolley, J.A. McNabb, and T.L. Mehlhorn, 1992. **Iron Dynamics: Transformation of Fe(II)/Fe(III) During Injection of Natural Organic Matter in a Sandy Aquifer.** Geochim. Cosmochim. Ac., 57, 1987-1999.

- McCarthy, J.F. and F.J. Wobber (Eds.), 1993. **Manipulation of Groundwater Colloids for Environmental Restoration**. Lewis Publishers, Boca Banton, pp 371.
- McCarthy, J.F. and J.M. Zachara, 1989. **Subsurface transport of contaminants**. *Environ. Sci. Technol.*, 23 (5), 496-502.
- McNeal, B.L. and N.T. Coleman, 1966. **Effect of Solution Composition on Soil Hydraulic Conductivity**. *Soil Sci. Soc. Am. J.*, 30, 308-312.
- Miller, W.P., H. Frenkel and K.D. Newman, 1990. **Flocculation Concentration and Sodium/Calcium Exchange of Kaolinitic Soil Clays**. *Soil Sci. Soc. Am. J.*, 54, 346-351.
- Mohan, K.K., M.G. Reed and H.S. Fogler, 1999. **Formation Damage in Smectite Sandstones by High Ionic Strength Brines**. *Colloid Surface A*, 154, 249-257.
- Mohan, K.K. and H.S. Fogler, 1997. **Colloidally Induced Smectite Fines Migration: Existence of Mikroquakes**. *AIChE J.*, 43 (3), 565-476.
- Mohan, K.K., 1996. **Water Sensitivity of Porous Media Containing Swelling Clays**. PhD Thesis, Chapter V.
- Mohan, K.K., R.N. Vaidya, M.G. Reed and H.S. Fogler, 1993. **Water Sensitivity of Sandstones containing Swelling and Non-Swelling Clays**. *Colloid Surface A*, 73, 237-254.
- Muecke, T.W., 1979. **Formation Fines and Factors Controlling Their Movement in Porous Media**. *J. Petrol. Technol.*, 31, 144-150.
- Newman, K.A. and K.D., Stolzenbach, 1996. **Kinetics of Aggregation and Disaggregation of Titanium Dioxide Particles and Glass Beads in a Sheared Fluid Suspension**. *Colloid Surface A*, 107, 189-203.
- Nightingale, H.I. and W.C. Bianchi, 1977. **Groundwater Turbidity Resulting from Artificial Recharge**. *Ground Water*, 15 (2), 146-152.
- Nocito-Gobel, J. and J.E. Tobiason, 1996. **Effects of Ionic Strength on Colloid Deposition and Release**. *Colloid Surface A*, 107, 223-231.
- Ochi, J. and J.-F. Vernoux, 1998. **Permeability Decrease in Sandstone reservoirs by Fluid Injection – Hydrodynamic and Chemical Effects**. *J. Hydrol.*, 208, 237-248.

- Penrose, W.R., W.L. Polzer, E.H. Essington, D.M. Nelson, and K.A. Orlandini, 1990. **Mobility of Plutonium and Americum through a Shallow Aquifer in a Semiarid Region.** Environ. Sci. Technol., 24 (2), 228-234.
- Puls, R.W. and R.M. Powell, 1992. **Transport of Inorganic Colloids Through Natural Aquifer Material: Implications for Contaminant Transport.** Environ. Sci. Technol., 26 (3), 614-621.
- Pupisky, H. and I. Shainberg, 1979. **Salt Effects on the Hydraulic Conductivity of a Sandy Soil.** Soil Sci. Soc. Am. J., 43 (3), 429-433.
- Quirk, J.P. and R.K. Schofield, 1955. **The Effect of Electrolyte Concentration on Soil Permeability.** J. Soil Sci., 6 (2), 163-178.
- Raveendran, P. and A. Amiratharajah, 1995. **Role of Short-Range Forces in Particle Detachment during Filter Backwashing,** J. Environ. Eng.-ASCE, 121 (12), 860-868.
- Roy, S.B. and D.A. Dzombak, 1996. **Colloid Release and Transport Processes in Natural and Model Porous Media.** Colloid Surface A, 107,245-262.
- Ryan, J. N., T.H. Illangasekare, M.I. Litaor and R. Shannon, 1998. **Particle and Plutonium Mobilization in Macroporous Soils during Rainfall Simulations.** Environ. Sci. Technol., 32 (4), 476-482.
- Ryan, J.N. and M. Elimelech, 1996. **Review: Colloid Mobilization and Transport in Groundwater.** Colloid Surface A, 107,1-56.
- Ryan, J.N. and P.M. Gschwend, 1994. **Effect of Solution Chemistry on Clay Colloid Release from an Iron Oxide-Coated Aquifer Sand.** Environ. Sci. Technol., 28 (9), 1717-1726.
- Saiers, J.E. and G.M. Hornberger, 1999. **The Influence of Ionic Strength on the Facilitated Transport of Cesium by Kaolinite Colloids.** Water Resour. Res., 35, (6), 1713-1727.
- Schroth, M., S.J. Ahearn, J.S. Selker and J.D. Istok, 1996. **Characterization of Miller Similar Silica Sands for Laboratory Hydrologic Studies.** Soil Sci. Soc. Am. J., 60 (5), 1331-1339.
- Shainberg, I., J.D. Rhoades, and R.J. Prather, 1981. **Effect of Low Electrolyte Concentration on Clay Dispersion and Hydraulic Conductivity of a Sodic Soil.** Soil Sci. Soc. Am. J., 45, 273-277.

- Sharma, M.M., H. Chamound, D.S.H. Sita Rama Sarma, and R.S. Schechter, 1991. **Factors Controlling the Hydrodynamic Detachment of Particles from Surfaces.** J. Colloid Interface Sci., 149, (1), 121-134.
- Snoeyink, V.L. and D. Jenkins, 1980. **Water Chemistry.** John Wiley and Sons, New York, pp 463.
- Stumm, W., 1992. **Chemistry of the Solid-Water Interface.** John Wiley and Sons, New York, pp 428.
- Suarez, D.L., J.D. Rhoades, R. Lavado, and C.M. Grieve, 1984. **Effect of pH on Saturated Hydraulic Conductivity and Soil Dispersion.** Soil Sci. Soc. Am. J., 48, 50-55.
- Vaidya R.N. and H.S. Fogler, 1990. **Formation Damage due to Colloidally Induced Fines Migration.** Colloid Surface A, 50, 215-229.
- Weisbrod, N., D. Ronen and R. Nativ, 1996. **New Method for Sampling Groundwater Colloids under Natural Gradient Flow Conditions.** Environ. Sci. Technol., 30, 3094-3101.
- Weisbrod, N., M. Niemet, M. Rockhold, T. McGinnis, and J.S. Selker, **Infiltration of Saline Solutions into variably saturated porous media, submitted, 2001.**
- Weisbrod, N., T. McGinnis, M. Niemet, and J.S. Selker, 2000. **Infiltration Mechanisms of Highly Saline Solutions and Possible Implications for the Hanford Site.** EOS Trans. AGU, 81 (48), Fall Meet. Suppl..
- Yan, Y.D., M. Borkovec & H. Sticher, 1995. **Deposition and Release of Colloidal Particles in Porous Media.** Prog. Coll. Pol. Sci., 98, 132-135.

## APPENDICES

**A APPENDIX A - SCANNING ELECTRON MICROSCOPY:  
PHOTOGRAPHS OF SEDIMENTS AND ATTACHED  
PARTICLES**

### A.1 Scanning Electron Microscopy

The three sediments (Silica Sand, Coarse and Fine Hanford Sediment) were studied with scanning electron microscopy (SEM). Sediment samples (untreated, after freshwater shock and acid washed) were put on aluminum specimen mounts and coated with carbon. Pictures were taken at various magnifications. Prints were made either on polaroid film (type 55) or as computer printouts. All Pictures were taken with an AmRay® 3300FE Field Emission Analytical Scanning Electron Microscope.



## A.2 The Silica Sand

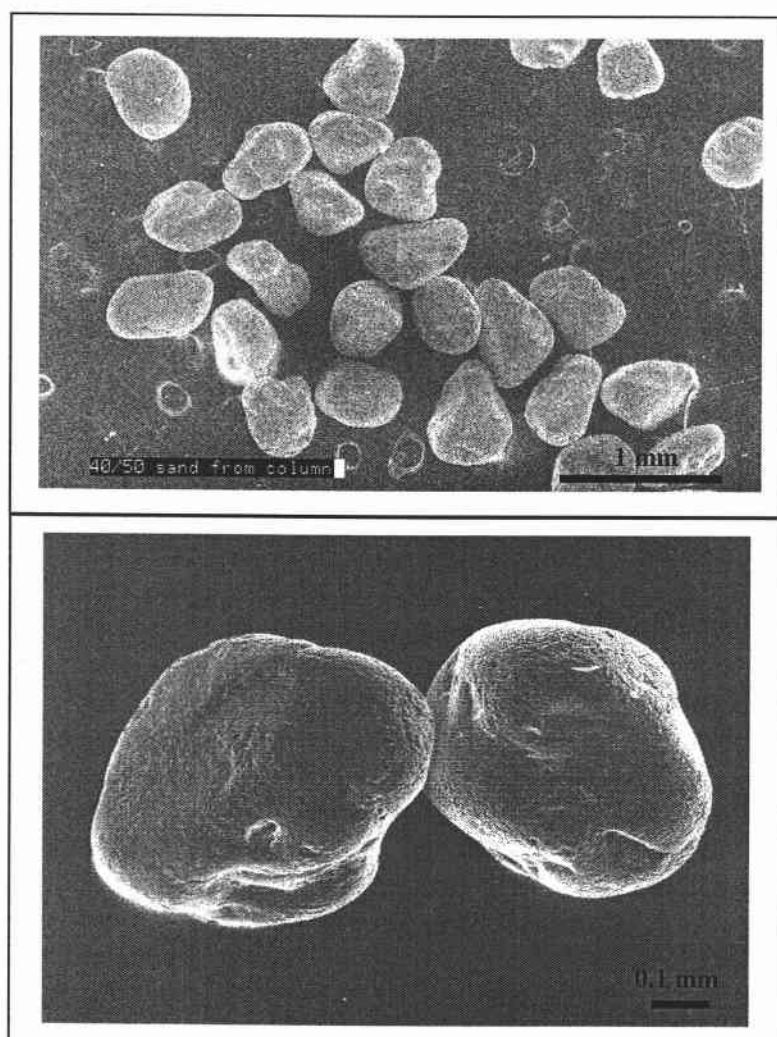


**Figure A.1** SEM pictures of Silica Sand (Accusand® 40/50).

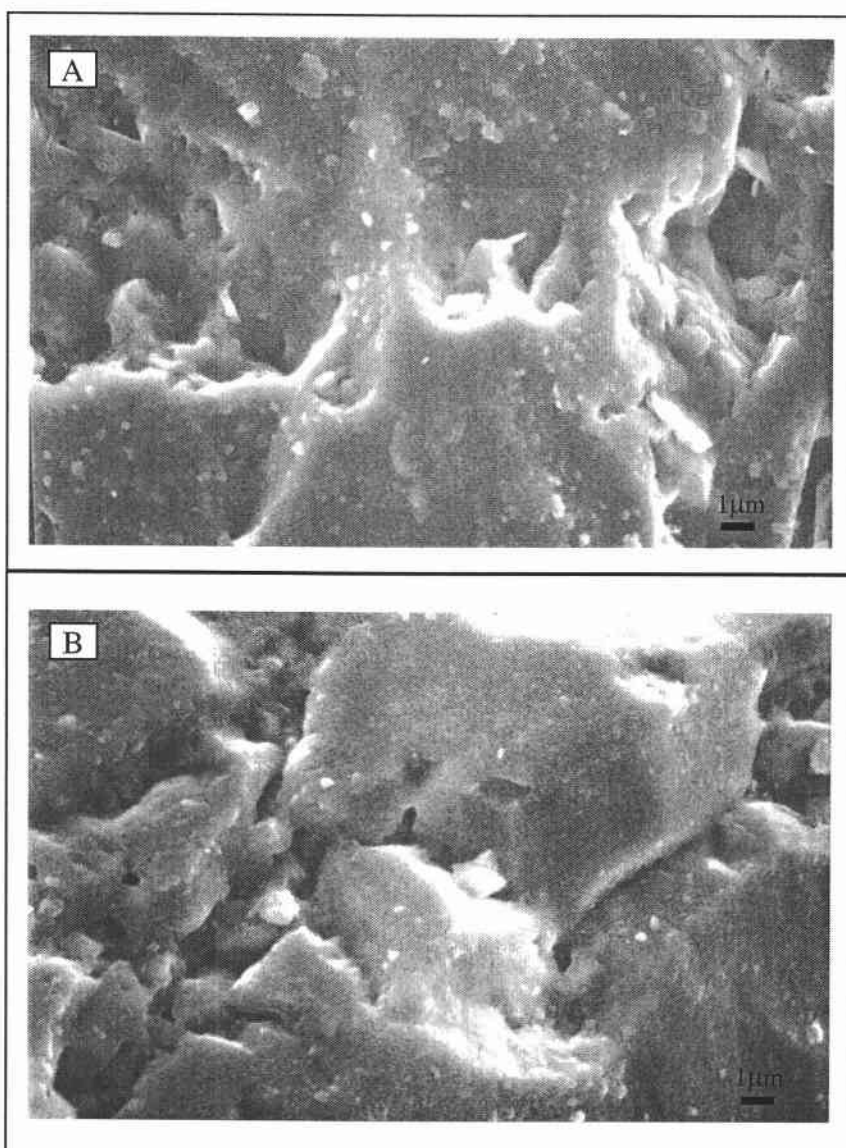


**Figure A.2** Surface of Silica Sand (Accusand® 40/50) before (A) and after (B) treatment with cycles of salt solution and deionized water. Note that fewer attached particles can be seen after the treatment.

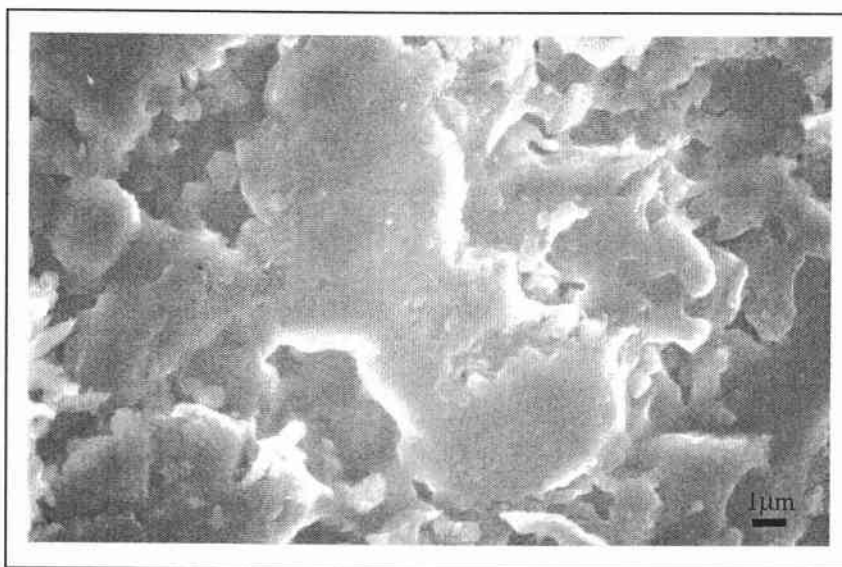


**Figure A.3** Surface of Silica Sand (Accusand® 40/50) after treatment with acid. Practically no particles remained attached.

### A.3 The Hanford Sediments

#### A.3.1 Coarse Sediment

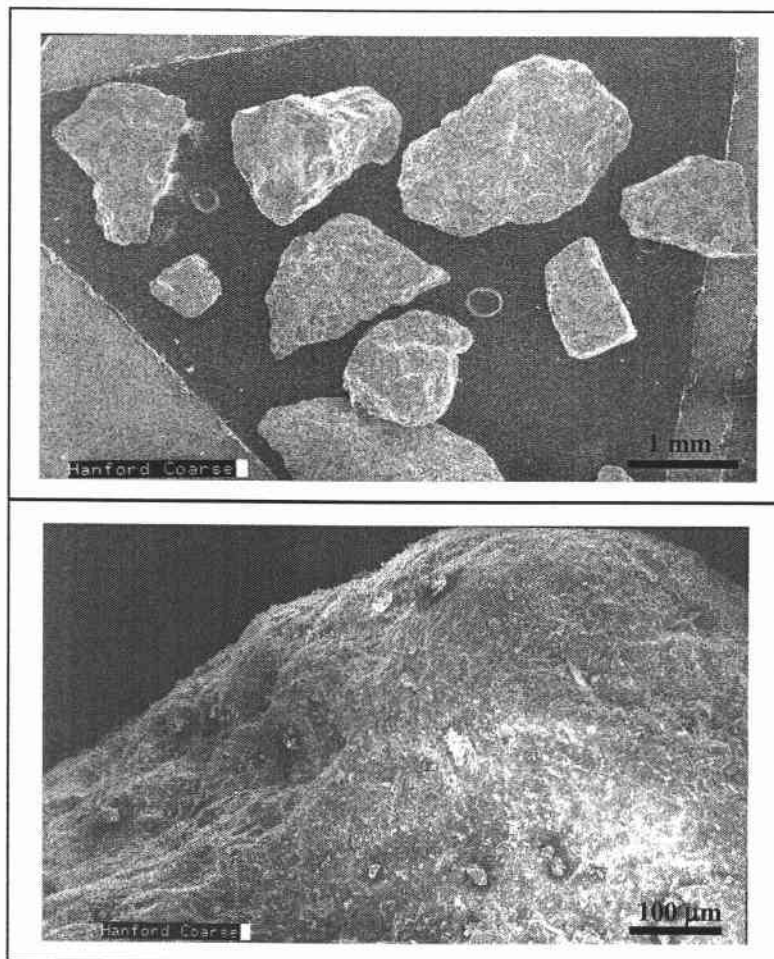


**Figure A. 4** Grains of the Coarse Hanford Sediment.

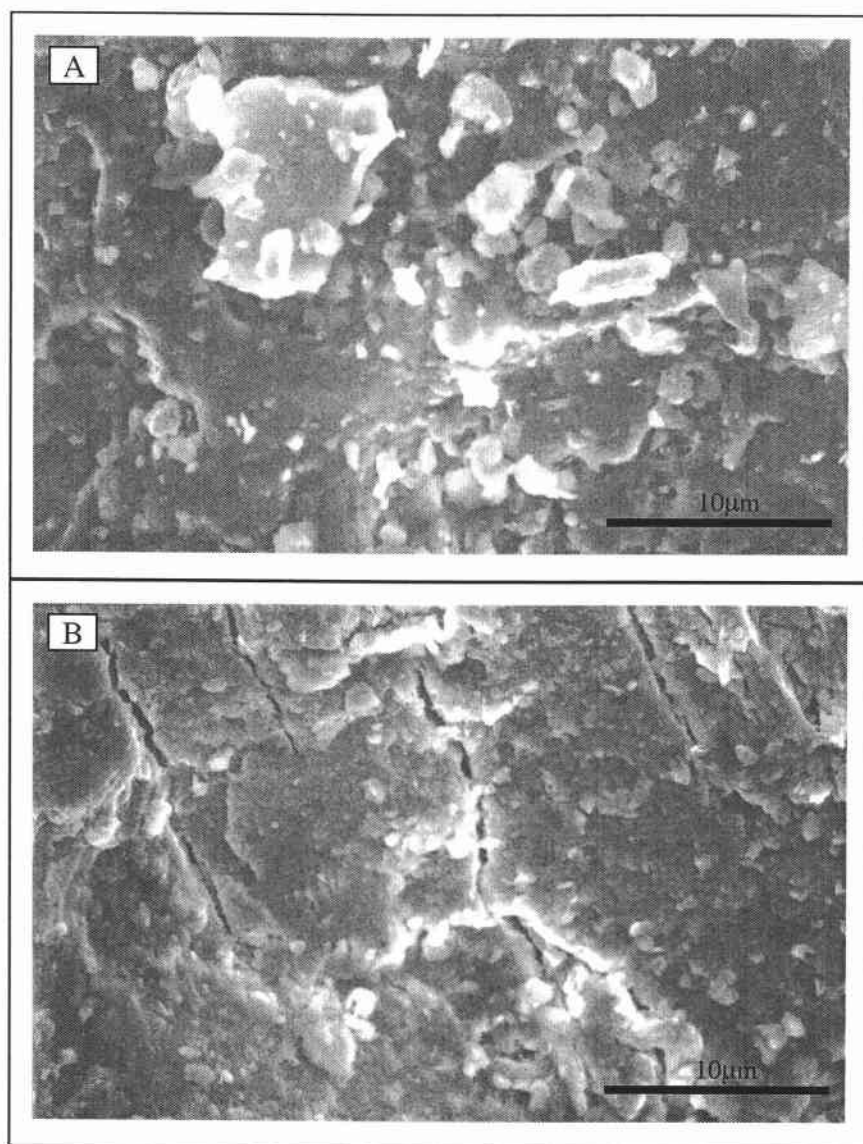


**Figure A. 5** Surface of Coarse Sediment before (A) and after (B) treatment with cycles of salt solution and deionized water. Note that fewer attached particles can be seen after the treatment.

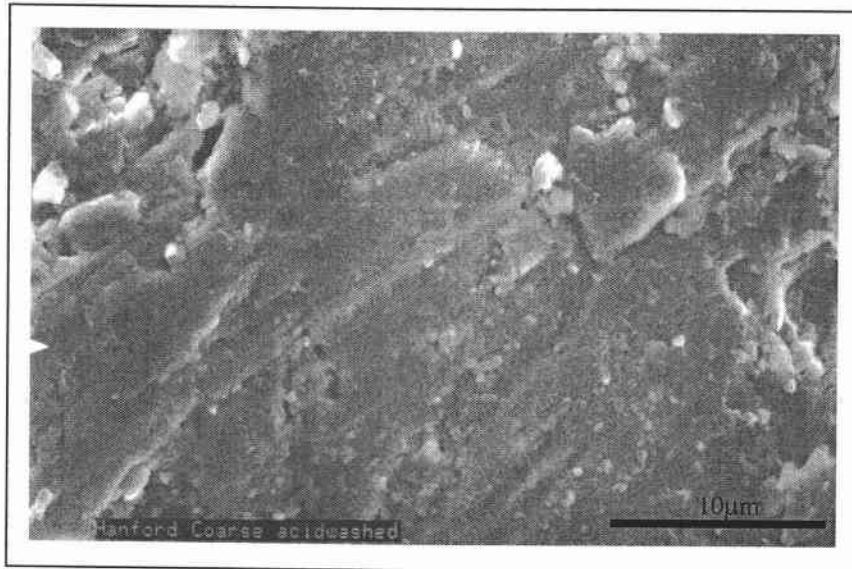


**Figure A. 6** Surface of Coarse Sediment after treatment with acid. Very few particles remained attached.

### A.3.2 Fine Sediment

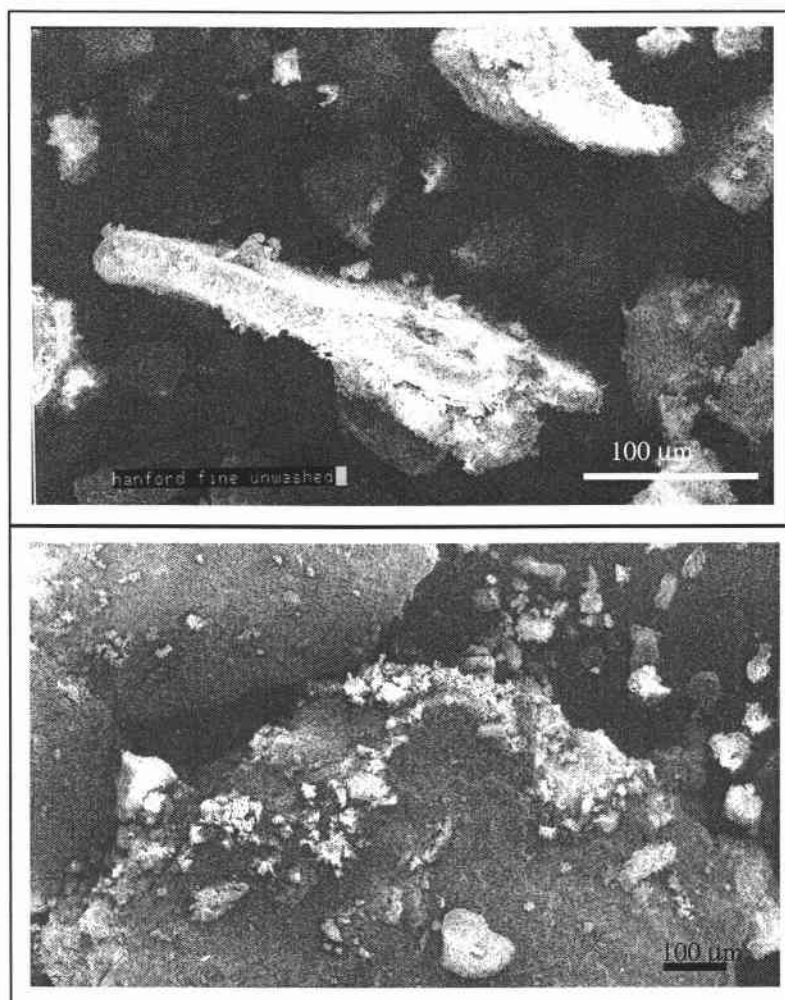


**Figure A. 7** Grains of Fine Hanford Sediment. Note the small size of most of the grains as well as the wide variability of grainsizes overall. Low image quality is due to electrostatic interferences.

**B    APPENDIX B - NUMERICAL SIMULATION OF  
PARTICLE RELEASE FROM SILICA SAND AS A  
RESULT OF SALINITY CHANGES**



## B.1 Introduction

In this study it was attempted to simulate the experiment described in the last paragraph of section 3.4. For simplification purposes the column was packed with Silica Sand (40/50 Accusand<sup>®</sup> grade) instead of the Hanford Sediments. High concentration salt solution (5 mol/l NaNO<sub>3</sub>) was applied alternating with deionized water during the lab experiment. Salt and particle concentrations were determined by measuring electro-conductivity and absorbance of the outflow, as described in Chapter 1. Particle release and deposition, as well as transport of both salt and released particles through the column, were simulated with a simple numerical model.

## B.2 Conceptual Model

Salt and particle breakthrough curves were simulated using a simple solute transport model. Questions of interest were the possibility to include terms of particle release and deposition into the solute transport model and the shape of the particle breakthrough curve.

As we are dealing with a column, a 1D model can be employed (**Figure B. 1**). The column used here is 20 cm long. Flow through the column is at steady state, but solute transport is transient. Relevant transport processes are advection and dispersion (diffusion is neglected).

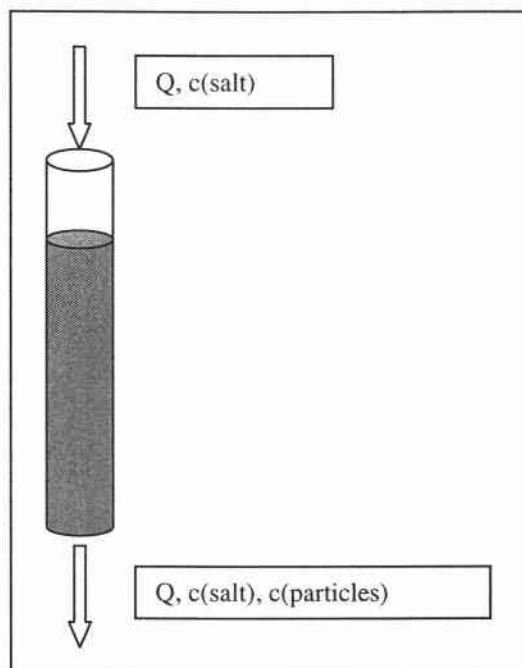


**Figure B. 1** Conceptual model

The retardation factor for the salt is set to be 1 as it is considered a conservative tracer. The particle retardation factor is assumed to be also equal to one. The material (silica sand) is assumed to be homogenous and isotropic. Initial conditions are as follows: (1) particle concentration in solution is zero; (2) initial salt concentration can be set by the user, the default choice is 0 mol/l. Constant head on both ends of the column is the governing boundary condition for flow. Head at the lower end of the column is equal to zero. Flow is constant over time. The boundary condition for the solute transport is determined by the inflow concentration, also a parameter, which can be set by the model user.

### B.3 Mathematical Model

#### B.3.1 Governing Equations

The governing differential equation for salt transport is the ADE (advection-dispersion-equation).

$$\frac{\partial C}{\partial t} = \frac{D}{R} \frac{\partial^2 C}{\partial x^2} - \frac{v}{R} \frac{\partial C}{\partial x} \quad (1)$$

Where  $C$  is concentration,  $t$  is time (min),  $D$  is the dispersion coefficient (cm),  $R$  is the retardation factor and  $v$  is the pore water velocity (cm/min). This equation was used to model the transport behavior of the salt solution.

For the case of the particles essentially the same equation was used but including a term for particle release/deposition. Retardation is assumed to be zero but can be fitted if necessary.

$$\frac{\partial C_p}{\partial t} = \frac{D_p}{R} \frac{\partial^2 C_p}{\partial x^2} - \frac{v_p}{R} \frac{\partial C_p}{\partial x} - \frac{1}{V} \frac{\partial S}{\partial t} \quad (2)$$

with the release/deposition term

$$\frac{1}{V} \frac{\partial S}{\partial t} = k_d C - \frac{1}{V} k_r S \quad (3)$$

$C$  is suspended concentration (mg/ml),  $t$  is time (min),  $D$  is the dispersion coefficient (cm),  $R$  is the retardation factor (1),  $v$  is pore water velocity (cm/min),  $V$  is volume (cm<sup>3</sup>),  $S$  is amount of particles available on the matrix (mg),  $k_d$  is the deposition rate and  $k_r$  is the release rate (1/s) (*Kretzschmar et al. 1999*).

### B.3.2 Implementation

Particle availability is assumed to be limited (400 mg over the whole column – experimental data) and release is assumed to decrease exponentially with particle availability. At salt concentrations above the CSC (0.02 mol/l - experimental data, Chapter 2) no particles are released and particles transported into a segment of higher salinity are subsequently deposited onto the matrix. This leads then to higher particle availability in this particular column segment. Below the CSC particle release is still also dependent on salt concentration: the lower the salt concentration, the higher the release. This corresponds to increasing repulsion forces between particles and matrix with decreasing salinity.

The resulting equation describing particle release is:

$$R = 0.012 \left( 1 - \frac{C_{salt}}{CSC} \right) \exp \left( 3 \left( 1 - \frac{\Sigma R}{R_{max}} \right) \right) \quad (4)$$

$R$  is the release per time step,  $R_{max}$  is the sum of available particles,  $\Sigma R$  is the sum of released particles of the previous time step,  $C_{salt}$  is the salt concentration. The values 0.012 and 3 are the fitting parameters obtained by optimizing the fit of the model to the experimental data.

Release and deposition of particles are implemented into the code as follows: **cnew** is the salt concentration at node  $i$ , **cpsum** is the sum of released particles at node  $i$ , and **cpnew** is the particle concentration (= number of particles) at node  $i$ . The



## B.4 The Model Interface

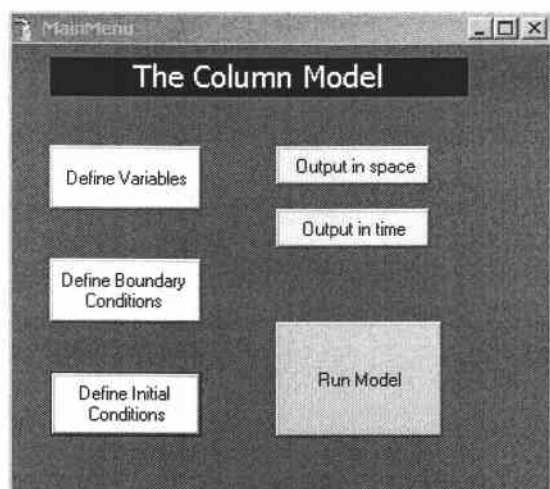
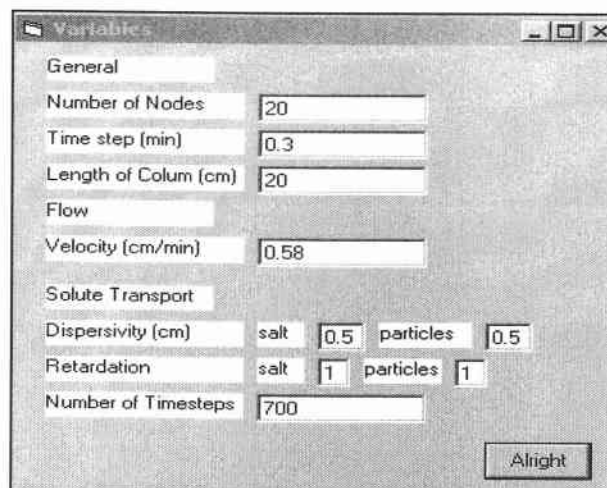


**Figure B. 2** Main menu

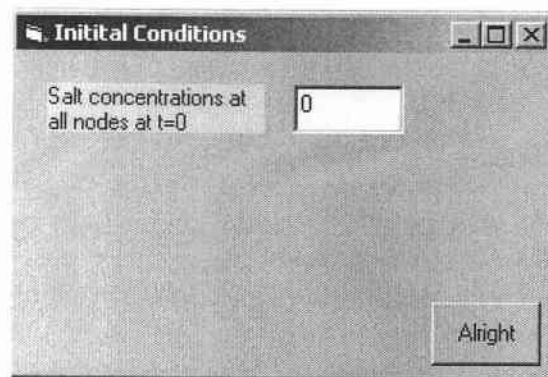
The model interface allows the user to set most of the important parameters (excluding particle availability and critical salt concentration). From the Main Menu window (**Figure B. 2**) you can open the input windows for general variables, initial and boundary conditions. By opening the output windows it is possible to watch particle and salt concentration throughout the column (output in space) or in the outflow (output in time) while the model is running. On the “Define Variables” window (**Figure B. 3**) the user can specify general parameters: number of nodes, length of the time-step, length of the column; flow parameters: velocity; parameters for solute transport: dispersivity and retardation and also the number of time-steps.



A screenshot of a software dialog box titled "Variables". It contains several input fields and buttons. The "General" section includes "Number of Nodes" (20), "Time step (min)" (0.3), and "Length of Colum (cm)" (20). The "Flow" section includes "Velocity (cm/min)" (0.58). The "Solute Transport" section includes "Dispersivity (cm)" with "salt" (0.5) and "particles" (0.5) sub-fields, "Retardation" with "salt" (1) and "particles" (1) sub-fields, and "Number of Timesteps" (700). An "Alright" button is at the bottom right.

General				
Number of Nodes	20			
Time step (min)	0.3			
Length of Colum (cm)	20			
Flow				
Velocity (cm/min)	0.58			
Solute Transport				
Dispersivity (cm)	salt	0.5	particles	0.5
Retardation	salt	1	particles	1
Number of Timesteps	700			

**Figure B. 3** Input of variables



A screenshot of a software dialog box titled "Initial Conditions". It contains a single input field for "Salt concentrations at all nodes at t=0" with the value 0. An "Alright" button is at the bottom right.

Initial Conditions	
Salt concentrations at all nodes at t=0	0

**Figure B. 4** Initial conditions

The user can also set the initial (salt concentration in the column at  $t=0$ ) (**Figure B. 4**) and boundary conditions (**Figure B. 5**). The boundary conditions are determined by selecting an inflow definition type. This can either be a constant

time interval of salt pulses or an instantaneous input (time and duration can be selected).

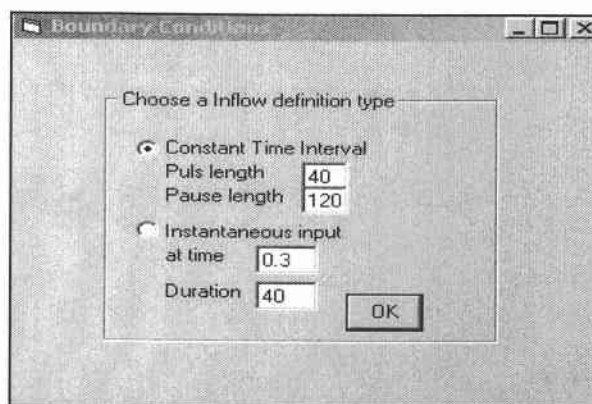


**Figure B. 5** Boundary Condition

## B.5 Model Validation/Verification

### B.5.1 Parameter Calibration for Salt Transport

Data and model output were compared for various dispersivities within the range characteristic for the 40/50 sands (0.3-0.5cm). The  $R^2$  values were calculated and the best fit determined.



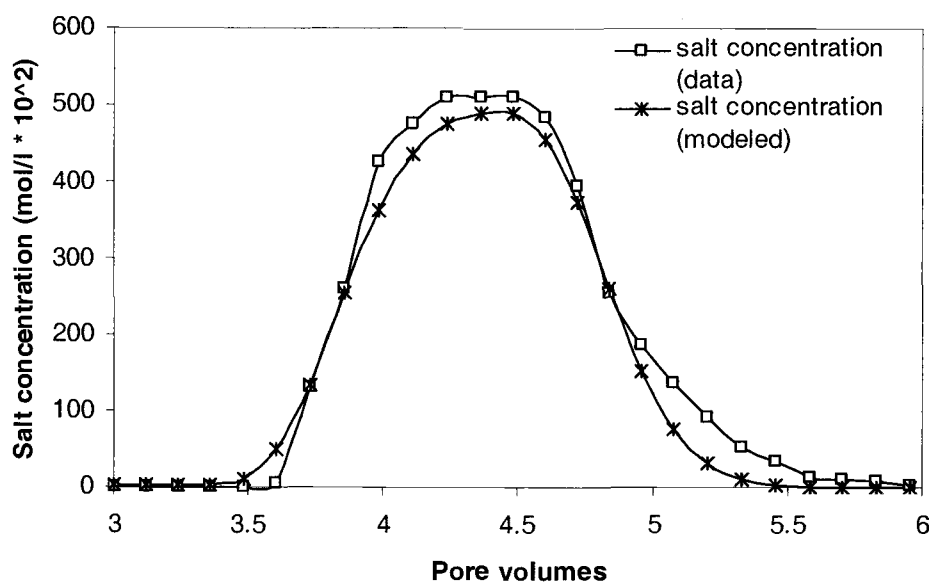


**Figure B. 6** Model and data of salt concentration in the outflow.

**Figure B. 6** shows the best fit out put of the salt transport model. The tail in salt concentration that appears in the data output cannot be explained by dispersion or retardation. It might be due to a reservoir within the system from where salt is not as easily removed. The dispersivity in this case is 0.5 cm and flow velocity 0.58 cm/min (measured velocity was about 0.5 cm/min). The resulting  $R^2$  value is 0.986. The obtained velocity and dispersivity was then also used for the particle transport model.

### B.5.2 Checking Model Dependence Upon Time Step and Number of Nodes

Changing the time-step ( $\Delta t$ ) or the number of nodes ( $\Delta x$ ) does not change the model output significantly (**Figure B. 7**).

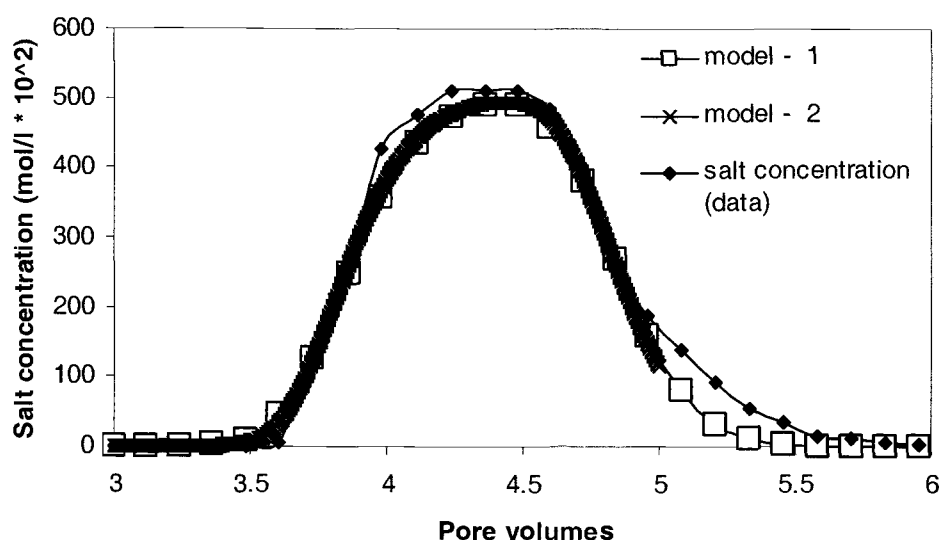


**Figure B. 7** Changing the time-step from 0.3 (model - 1) to 0.08 (model - 2) and the number of nodes from 20 (model - 1) to 80 (model - 2) does not change the output significantly. Simulation was halted at 5 pore volumes due to computational limitations.

### B.5.3 The Particle Model

Mass balance calculations on the particle simulations showed that the 400 mg of available particles in the column are fully recovered in the outflow. The output of the particle model matched the data surprisingly well (**Figure B. 8**). This

suggests that critical salt concentration and particle availability are major factors in the particle release function. The fact that modeled particle release precedes the measured values by a fraction of a pore volume is due to the fact that salt concentrations in the model drop earlier, as the tail of salt solution that can be seen in the data is not accounted for in the simulation.

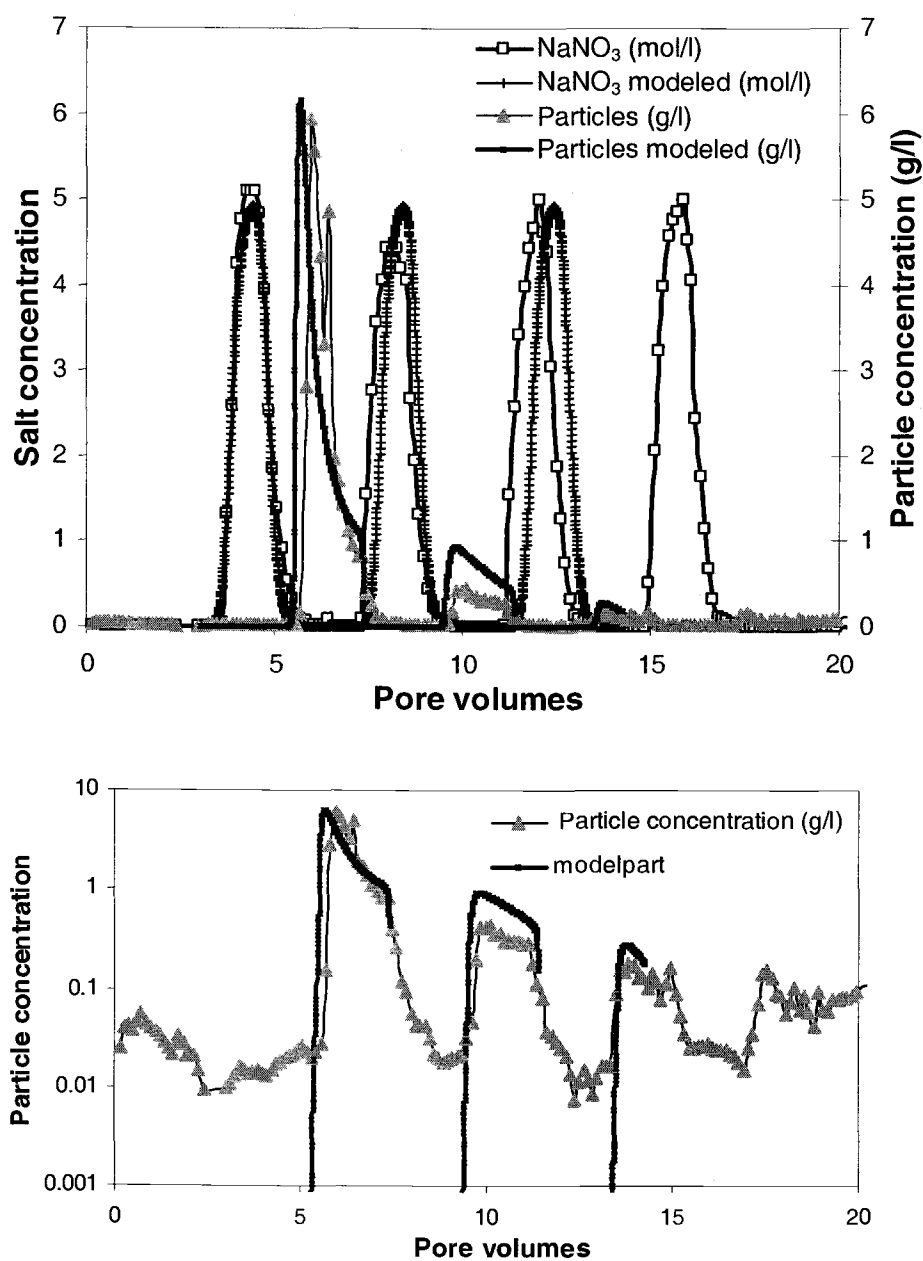


**Figure B. 8** Comparison of model output with measured data

## B.6 Conclusions

Overall, this simple model worked surprisingly well. Salt transport was described reasonably well with the advection dispersion equation. The exponential function used to express release within the column and the included deposition term are able to capture the general behavior of particle release. However, the model could be improved by finding physically based parameters to replace the fitting parameters. The user-friendly interface simplifies parameter input.

## B.7 References

- Kretzschmar, R., M. Borkovec, D. Grolimund and M. Elimelech., 1999. **Mobile Subsurface Colloids and Their Role in Contaminant Transport.** Adv. Agron., 66, 121-193.